Journal of Magnetic Resonance 212 (2011) 330–343

Contents lists available at ScienceDirect

Journal of Magnetic Resonance

journal homepage: www.elsevier.com/locate/jmr

CPMG echo amplitudes with arbitrary refocusing angle: Explicit expressions, asymptotic behavior, approximations

M.V. Petrova [a,b,*], A.B. Doktorov [c], N.N. Lukzen [a]

[a] International Tomography Center SB RAS, Institutskaya 3a, Novosibirsk 630090, Russia
[b] Novosibirsk State University, Novosibirsk 630090, Russia
[c] Institute of Chemical Kinetics and Combustion SB RAS, Institutskaya 3, Novosibirsk 630090, Russia

ARTICLE INFO

Article history:
Received 15 April 2011
Revised 8 July 2011
Available online 27 July 2011

Keywords:
CPMG sequence
Spin echo
Asymptotic form

ABSTRACT

Exact explicit analytical expression for echoes in the Carr–Purcell–Meiboom–Gill sequence with arbitrary excitation and refocusing angles and resonance offset of RF pulses was obtained, employing the generating functions formalism developed earlier by authors. Asymptotic form and analytical approximation for echoes were derived in an elegant way and analyzed in details. In particular, it was shown that depending on T_1, T_2 and parameters of the pulse sequence, oscillatory behavior of echoes can take place. Accuracy of asymptotic forms and approximations were tested by comparison with exactly calculated echo amplitudes. Besides, it was shown, that the generating function approach can be applied to the consideration of terminated pulse sequences, when after-pulses echoes are registered.

1. Introduction

Magnetic Resonance Imaging (MRI) is widely used in medical and biological research. At the same time the method shows promise for studying chemical reactions in situ [1], fluxes, mass transfer process [2], material structure and properties [1–3]. Long trains of periodic RF pulses make an integral part of NMR and MRI methods.

Echo pulse sequences conventionally used in MR imaging contain π and $\pi/2$ resonant RF pulses that are primarily chosen for the simpler data analysis. For instance, the classic Carr–Purcell–Meiboom–Gill (CPMG) pulse sequence

$$(\pi/2)_{-y} - TE/2 - \pi_x - TE - \pi_x - TE - \pi_x - \cdots \tag{1}$$

(TE is echo time (inter-pulse period), subscripts "$-y$" and "x" denote the pulse phase) consists of $\pi/2$ excitation pulse and π refocusing pulses. However, it is known that any refocusing pulse can produce spin echoes [4,5]. Moreover, using smaller flip angle of the RF pulse appears to be an actual problem in MRI since it can permit one to decrease full scanning time [6], does not demand preliminary time-consuming calibration of the RF probe, and permits one to decrease the RF load. Understanding echoes in any flip angle regime is also actual for NMR logging [7].

The response of the CPMG sequence has been heavily studied [4,5,8–11]. Some of these approaches involve the eigenvalues analysis of the operators of evolution of the magnetization vector [9,10], others rest on direct calculation of the magnetization by the recursion [8,11] or consider the asymptotic regime only [10]. Most of these approaches uses numerical methods, and they lack a closed form expression for echo signal. However, possession of an analytical expression is an important point, since it allows one to get a deeper insight into the nature of the signal formation. Nevertheless, a direct laborious derivation of an analytical form of echo from the Bloch equations has not been performed so far.

To this end, earlier we proposed and developed a new general approach for analysis of spin system response to a periodic pulse train with arbitrary excitation and refocusing flip angle and resonance offset [12,13]. This approach is based on the generation functions (GF) formalism, which is very known in mathematics [14], and allowed us to obtain analytical results in an elegant way. The essence of the formalism is as follows. If one has a number series (infinite in a general case) $M_1, M_2 \ldots, M_n, \ldots$, then the corresponding GF is the following function of a complex variable z:

$$f(z) = M_0 + M_1 z + \cdots + M_n z^n + \cdots = \sum_{n=0}^{\infty} M_n z^n, \tag{2}$$

where $|z| < 1$, which usually ensures the convergence of the series. Thus, the GF comprises complete information about all values M_n at once. The advantage of the GF approach is that the GF often has a simple analytical form, whereas the explicit expression for M_n cannot be obtained analytically or is very cumbersome. For instance, the form of the generating function for Legendre polynomials

$$f(z) = \sum_{k=0}^{\infty} P_k(x) z^k = \frac{1}{\sqrt{1 - 2xz + z^2}} \tag{3}$$

is much simpler than that for the polynomials.

* Corresponding author at: International Tomography Center SB RAS, Institutskaya 3a, Novosibirsk 630090, Russia. Fax: +7 383 333 13 99.
E-mail address: petrovamv@tomo.nsc.ru (M.V. Petrova).

1090-7807/$ - see front matter © 2011 Elsevier Inc. All rights reserved.
doi:10.1016/j.jmr.2011.07.013

Taking $z = e^{i\vartheta}$ ($0 \leqslant \vartheta < 2\pi$) or $z = e^{-s}$ ($s > 0$), one can see that GF is actually a discrete Fourier or Laplace transform of the M_n series. Therefore, M_n can be calculated easily using conventional Fourier transformation of the GF. One can consider echo amplitudes in the CPMG pulse sequence as the values M_n (hereafter by the term "echo amplitude" we mean the net complex magnetization $M^+ = M_x + iM_y$ at the moment of the echo). GFs for echoes induced by various periodic pulse sequences can then be tabulated as it is done for Fourier or Laplace transformations of various functions.

In Refs. [12,13] we obtained analytically the GFs for echo amplitudes in the CPMG sequence with resonant and nonresonant RF pulses with arbitrary refocusing angle, respectively. The asymptotic form for echo amplitudes in case of equal spin relaxation times $T_1 = T_2$ was also found [12,13].

The study of the asymptotic behaviour from our point of view is important to better understand the general properties of the CPMG sequence, and besides, the asymptotic form allows one to easily obtain the information about T_1 and T_2 relaxation times using experimental echoes with large numbers. Other reasons come from NMR logging where due to the wide distributions of static and RF magnetic fields, the asymptotic behavior is quickly reached [10]. However, it turns out that for some relation between relaxation times and refocusing angle α echo asymptotic form shows good agreement with the exact one only for very large numbers of echoes. Thus, an actual task arises to obtain analytical approximations which are relatively simple and work well for transient echoes.

In the present work we employ the GF, obtained earlier, to derive explicit expressions for the echo amplitudes, their asymptotic behavior and analytical approximations for them for arbitrary T_1 and T_2.

In what follows, the diffusion effects are neglected, the RF pulse effect is treated as instantaneous rotation of the magnetization vector, spin relaxation during the pulse is neglected.

The paper is organized as follows. In Section 2, we consider the GF for a definite isochromat in the CPMG sequence and apply the configuration approach to it. In Section 3 MRI CPMG pulse sequence is considered, when a linear magnetic field gradient is switched on between the pulses only. It is shown, that in this case averaging over inhomogeneous broadening, induced by the gradient, can be easily performed immediately in the GF. Some comments on terminated MRI pulse sequences are also made. Applicability of the GF approach to NMR logging is discussed in Section 4. In Section 5 exact expression for MRI CPMG echoes are derived. It is shown, that the echo amplitudes can be expressed in terms of the well-known Legendre polynomials. In Section 6 the asymptotic behavior of echoes is determined. It is shown, that four cases for the asymptotic regime can be distinguished. In Section 7 analytical approximations for echo amplitudes are presented. In particular, it is shown that depending on T_1, T_2 and parameters of the pulse sequence, oscillatory behavior of echoes can take place. Analysis of accuracy of the asymptotic form and analytical approximation is performed in Section 8.

2. Generating function for a definite isochromat in the CPMG sequence. The Configuration approach

Let us consider the CPMG pulse sequence with arbitrary refocusing angle α. The pulses are allowed to be off resonance, and $\Delta\omega$ is the resonance offset for a given voxel. The corresponding GF for the magnetization of a definite isochromat is defined by Eq. (6) of Ref. [13]. If $M_0^+ = M_{x0} + iM_{y0} = M_{eq}m_0^+$, $M_0^- = M_{x0} - iM_{y0} = M_{eq}m_0^-$ and $M_{z0} = m_{z0}M_{eq}$ are the magnetization components just after the excitation pulse, and M_{eq} is the equilibrium magnetization, then the GF for the transverse magnetization $M^+ = M_x + iM_y$ of a certain isochromat has the following form:

$$\frac{f(z)}{M_{eq}} = \frac{D_0 m_0^+ + Q_1 U + Q_2 U^2 + Q_3 U^3}{D_0 + D_1 U^2 + D_2 U^4}, \tag{4}$$

where

$$Q_1 = z\xi_2 \frac{\lambda^*}{\lambda} Q_3 = 2z^2 \xi_2^{3/2} \mu \lambda^* \left[\frac{1 - z\xi_1}{1 - z} - \xi_1^{1/2}(1 - m_{z0}) \right], \tag{5}$$

$$Q_2 = [1 - z\xi_1(|\lambda|^2 - \mu^2)]m_0^+ + z\xi_2 \mu^2 (1 + z\xi_1) m_0^-, \tag{6}$$

$$D_0 = \left(\frac{\lambda^*}{\lambda}\right)^2 D_2 = z\xi_2 \lambda^{*2}(1 - z\xi_1), \tag{7}$$

$$D_1 = 1 - z^3 \xi_1 \xi_2^2 - z(\xi_1 - z\xi_2^2)(|\lambda|^2 - \mu^2), \tag{8}$$

$$\lambda = \sin\varphi \sin\frac{\alpha}{2} + i\cos\frac{\alpha}{2}, \tag{9}$$

$$\mu = \cos\varphi \sin\frac{\alpha}{2}, \tag{10}$$

$$U = e^{-i\psi}, \tag{11}$$

and star denotes complex conjugation. Here

$$\alpha = \omega_1 \tau \sqrt{1 + (\Delta\omega/\omega_1)^2}, \tag{12}$$

$$\varphi = \arctan(\Delta\omega/\omega_1), \tag{13}$$

$\omega_1 = \gamma B_1$, B_1 is RF field amplitude, τ is the refocusing pulse duration, i.e., $\omega_1\tau$ is the nominal refocusing angle; γ is the nucleus gyromagnetic ratio, $\xi_{1,2} = \exp\{-TE/T_{1,2}\}$, T_1 and T_2 are spin–lattice and spin–spin relaxation times, respectively, TE is echo time (inter-pulse period), and ψ is the phase accumulated during one half of the inter-pulse period for a definite isochromat.

As was mentioned in Ref. [13], the magnetization of a certain isochromat can be represented in the following form:

$$M_n^+(\omega_1, \Delta\omega, U) = \sum_{k=-2n}^{2n} K_{nk}(\omega_1, \Delta\omega) U^k, \tag{14}$$

$K_{n-2n} = K_{n-2n+1} = 0$ for $n \neq 0$, that is actually a decomposition of the magnetization into the so-called configurations [5]. Therefore, the GF (4) for a definite isochromat can also be decomposed into the configurations:

$$f(z) \equiv f(z, \omega_1, \Delta\omega, U) = \sum_{n=0}^{\infty} M_n^+(\omega_1, \Delta\omega, U) z^n$$
$$= \sum_{k=-\infty}^{+\infty} F_k(z, \omega_1, \Delta\omega) U^k, \tag{15}$$

where the kth configuration

$$F_k(z, \omega_1, \Delta\omega) = \sum_{n \geqslant |k|/2}^{\infty} K_{nk}(\omega_1, \Delta\omega) z^n \tag{16}$$

depends on the pulse parameters only, while fast oscillating factor U^k is determined by the resonance offset between pulses, which can be different from that during the pulse (for instance, because of application of a magnetic field gradient).

Exact explicit analytical expression for $M_n^+(\omega_1, \Delta\omega, U)$ of a definite isochromat can be obtained from Eq. (4), but the final expression is a multiple sum, which is very cumbersome, and will not be presented here.

3. Generating function for CPMG echo amplitudes in MRI

In MRI pulse sequences a linear magnetic field gradient $\vec{\mathbf{G}}$ is switched on between the pulses only, therefore,

$$\psi = \psi_{MRI}(\vec{\mathbf{r}}) = (\Delta\omega + \gamma\vec{\mathbf{G}}, \vec{\mathbf{r}})\frac{TE}{2}, \tag{17}$$

and if the range of ψ_{MRI} is wide enough, averaging over inhomogeneous broadening (isochromats) induced by the magnetic field gradient, is reduced to the consideration of the null-configuration $F_0(z, \omega_1, \Delta\omega)$ in Eq. (15) only, that tremendously simplifies the GF form.

For the MRI CPMG pulse sequence with arbitrary refocusing angle α, and the excitation pulse angle is not necessarily equal to $\pi/2$, the null-configuration $F_0(z, \omega_1, \Delta\omega)$, which is actually the GF for CPMG echo amplitudes M_n^+ in MRI, was determined in Ref. [13]:

$$F_0(z) = \sum_{n=0}^{\infty} M_n^+ z^n = \frac{M_{x0}}{2}\left[1+\sqrt{\frac{X}{Y}}\right] + i\frac{M_{y0}}{2}\left[1+\sqrt{\frac{Y}{X}}\right],$$
$$X = (1+z\xi_2)[1 - z(\xi_1+\xi_2)(\cos\alpha\cos^2\varphi + \sin^2\varphi) + z^2\xi_1\xi_2], \quad (18)$$
$$Y = (1-z\xi_2)[1 - z(\xi_1-\xi_2)(\cos\alpha\cos^2\varphi + \sin^2\varphi) - z^2\xi_1\xi_2],$$

where all notations are defined in the previous section. Quantities M_{x0} and M_{y0} are the x and y components of the initial magnetization vector $\vec{M}_0$ just after the excitation pulse, respectively:

$$M_{x0} = M_{eq}\cos\varphi\sin\left(\omega_1\tau_1\sqrt{1+(\Delta\omega/\omega_1)^2}\right),$$
$$M_{y0} = -M_{eq}\sin 2\varphi\sin^2\left(\frac{\omega_1\tau_1}{2}\sqrt{1+(\Delta\omega/\omega_1)^2}\right), \quad (19)$$

where τ_1 is the excitation pulse duration, and $\omega_1\tau_1$ is the nominal excitation angle. The parameters of the excitation pulse are only manifested in this initial condition for the transverse magnetization. Therefore, actually the GF (18) describes both the CPMG and CP (Carr–Purcell) pulse sequences, as well as the sequences with arbitrary phase of the excitation pulse (one should choose the appropriate initial condition). Moreover, as was shown in Ref. [13], Eq. (18) can be extended to the echo-sequence with phase cycling of the refocusing pulses (i.e., when the phase of the nth refocusing pulse is $(n-1)\phi$), if values M_n^+ in Eq. (18) are regarded now as $e^{i(n-1/2)\phi}M_n^+$, where M_n^+ is the net transverse magnetization as before. For example, at $\phi = \pi$, i.e., when the x and $-x$ phases of the refocusing pulses are alternated, the CPMG sequence turns in fact to the CP one and vice versa, that corresponds to the results presented in Ref. [15].

It follows from the form of the GF (18), that nonresonant case ($\Delta\omega \neq 0$) can be reduced to the resonant one ($\Delta\omega = 0$) with redefined refocusing angle α_e:

$$\cos\alpha_e = \cos\alpha\cos^2\varphi + \sin^2\varphi, \quad (20)$$

i.e., one can consider the sequence consisting of nonresonant pulses as the resonant pulse train with refocusing angle α_e. This interesting result was first obtained in Ref. [16] and naturally follows from the GF form [13]. Thereby, henceforth, when considering infinite pulse sequences, i.e., when the refocusing pulse precedes the echo signal, we will address only to resonant RF pulse case.

3.1. After-pulses echoes

The original GF (4) for a definite isochromat comprises a complete information about all configurations and their contributions to echoes at once. Hence, it permits one to solve even a more general problem, when the pulse sequence is terminated after the mth refocusing pulse, and the after-pulses echoes M_{nm}^+ are registered at the time points $t = (m + \frac{n}{2}) \times TE$, provided that the same periodic scheme for magnetic field gradient is continued:

$$F_{-n}(z, \omega_1, \Delta\omega) \equiv F_{-n}(z) = \xi_2^{-n/2}\sum_{m=0}^{\infty} M_{nm}^+ z^m, \quad (21)$$

i.e., the nonnull-configurations of the GF (4) are actually the GFs for after-pulses echo amplitudes, i.e. for magnetization averaged over isochromats at the moment of the echo. The expression for $F_{-n}(z)$ can be obtained by integration of $f(z, U)U^{n-1}$ over variable U along the unity circle contour in the complex plane. The final expressions for $F_{-n}(z)$, $n = 0, \pm1, \ldots$, are as follows:

$$F_{-2k}(z) = [U_1(z)]^k\left[F_0(z) - (1-\delta_{k0})M_0^+\right], \quad (22)$$

and

$$F_{-2k+1}(z) = z\xi_2^{1/2}\frac{\mu}{\lambda^*}[U_1(z)]^k\left[\frac{1}{1-z} - \xi_1^{1/2}\frac{1-m_{z0}}{1-z\xi_1}\right][2\delta_{k0} - 1$$
$$+\frac{(1-z^2\xi_2^2)(|\lambda|^2 - \mu^2 - z\xi_1)}{\sqrt{XY}}\Bigg], \quad (23)$$

where

$$U_1(z) = -\frac{D_1}{2D_2} + \frac{\sqrt{XY}}{2D_2}, \quad (24)$$

and $F_0(z)$, X and Y are defined in Eq. (18); note, that X, Y, D_1 and D_2 are also functions of z.

4. Generating function for CPMG echo amplitudes in NMR logging

In NMR logging, in contrast to MRI pulse sequences, a certain isochromat has the same resonance offset $\Delta\omega = \Delta\omega(\vec{\mathbf{r}})$ during both the pulse and the inter-pulse period, and phase incursion for a half of the inter-pulse period for a definite isochromat is now

$$\psi = \psi_{Logging}(\vec{\mathbf{r}}) = \Delta\omega(\vec{\mathbf{r}})\frac{TE}{2}. \quad (25)$$

Thus, $\Delta\omega$ is the same for both $F_k(z, \omega_1, \Delta\omega)$ and U^k in Eq. (15), and averaging over different isochromats cannot be directly performed by simple exclusion of the terms with $k \neq 0$ (the nonnull-configurations), but the complete GF (4) should be weighted with the ω_1 and $\Delta\omega$ distribution $s(\omega_1, \Delta\omega)$ and integrated:

$$F_{\text{echo}}(z) = \int\int f\left(z, \omega_1, \Delta\omega, e^{-i\frac{TE}{2}\Delta\omega}\right)s(\omega_1, \Delta\omega)\,d\omega_1\,d\Delta\omega \quad (26)$$

(index "echo" denotes the GF for the net echo signal). Nevertheless, we suppose even in this case the GF (4) for a definite isochromat strongly simplifies the computation process, since averaging over $\Delta\omega$ and ω_1 can be performed in the GF at once.

Moreover, the coefficients $F_k(z, \omega_1, \Delta\omega)$ in Eq. (15) are some functions of $\Delta\omega/\omega_1$ and $\sqrt{1+(\Delta\omega/\omega_1)^2}$ and depend weakly on the offset $\Delta\omega$ compared to fast oscillating factor $e^{-ik\Delta\omega TE/2}$. Therefore, even in this case the nonull-configuration contributions in Eq. (26) can be omitted to a high accuracy, if the width Γ of $\Delta\omega$-distribution is wide enough:

$$\frac{1}{4\pi}\Gamma \times TE \gg 1. \quad (27)$$

Then, in Eq. (26) one can use the function (18) instead of $f\left(z, \omega_1, \Delta\omega, e^{-i\frac{TE}{2}\Delta\omega}\right)$, that was verified numerically for homogeneous (rectangular) and gaussian $\Delta\omega$-distributions.

For the same reason for the terminated pulse sequences only the corresponding configuration $F_{-n}(z)$ can be considered.

5. Exact expression for MRI CPMG echo amplitudes

In what follows, we consider infinite MRI CPMG pulse sequences, i.e., the refocusing pulse precedes the echo signal. The corresponding GF for echo amplitudes is determined by Eq. (18), and from now on, the index "0" will be omitted. Since echo amplitudes $M_n^+ = M_{xn} + iM_{yn}$ are the coefficients preceding z^n in power expansion of GF

$$F(z) = \sum_{n=0}^{\infty} M_n^+ z^n,$$

it is obvious that the nth echo amplitude can be obtained as

$$M_n^+ = \frac{1}{n!}\frac{d^n}{dz^n}F(z)\bigg|_{z=0}. \quad (28)$$

Another expression for M_n^+ in the integral form can readily be derived from the theory of functions of a complex variable:

$$M_n^+ = \frac{1}{2\pi i}\oint F(z)\frac{dz}{z^{n+1}}. \tag{29}$$

In Refs. [12,13] it has been shown that at equal spin relaxation times $T_1 = T_2$ ($\xi_1 = \xi_2 = \xi$) the echo amplitudes can be represented as the sum of Legendre polynomials:

$$M_{xn} = \frac{M_{x0}\xi^n}{2}\left[\delta_{n0} + P_n(\cos\alpha) - P_{n-1}(\cos\alpha) + 4\sin^2\frac{\alpha}{2}\sum_{k=0}^{n-1}P_k(\cos\alpha)\right], \tag{30}$$

$$M_{yn} = \frac{M_{y0}\xi^n}{2}[\delta_{n0} + P_n(\cos\alpha) - P_{n-1}(\cos\alpha)].$$

Eq. (30) was obtained by straight-forward expansion of GF

$$F(z)|\xi_1 = \xi_2 = \frac{M_{x0}}{2}\left[1 + \frac{\sqrt{1 - 2\xi z\cos\alpha + \xi^2 z^2}}{1 - \xi z}\right] + i\frac{M_{y0}}{2}\left[1 + \frac{1 - \xi z}{\sqrt{1 - 2\xi z\cos\alpha + \xi^2 z^2}}\right], \tag{31}$$

in a power series in z, employing the GF for Legendre polynomials (Eq. (3)).

In a similar way the general case $T_1 \neq T_2$ can be considered, and the exact expression for echoes can be found. To do this, let us rewrite Eq. (18) as

$$F(z) = \frac{M_{x0}}{2}\left[1 + \frac{X}{\sqrt{XY}}\right] + i\frac{M_{y0}}{2}\left[1 + \frac{Y}{\sqrt{XY}}\right]. \tag{32}$$

Using Eq. (3), one can represent $1/\sqrt{XY}$ as follows:

$$\frac{1}{\sqrt{XY}} = \sum_{k,l,m=0}^{\infty} P_k\left(\frac{\xi_1 + \xi_2}{2\sqrt{\xi_1\xi_2}}\cos\alpha\right)P_m\left(\frac{\xi_1 - \xi_2}{2i\sqrt{\xi_1\xi_2}}\cos\alpha\right) \times P_l(0)i^{l+m}(\xi_1\xi_2)^{\frac{k+m}{2}}\xi_2^l z^{k+l+m}. \tag{33}$$

Substituting this expression in Eq. (32) and collecting the coefficients preceding the same power of z, one obtains

$$\frac{M_{xn}}{M_{x0}} = \frac{(\xi_1\xi_2)^{n/2}}{2}[\delta_{n0} + (S_n + \chi S_{n-1}) - \cos\alpha(\chi^{-1} + \chi)(S_{n-1} + \chi S_{n-2}) + (S_{n-2} + \chi S_{n-3})],$$
$$\frac{M_{yn}}{M_{y0}} = \frac{(\xi_1\xi_2)^{n/2}}{2}[\delta_{n0} + (S_n - \chi S_{n-1}) - \cos\alpha(\chi^{-1} - \chi)(S_{n-1} - \chi S_{n-2}) - (S_{n-2} - \chi S_{n-3})], \tag{34}$$

where

$$S_n = \sum_{0\leqslant k+2p\leqslant n} P_k\left(\frac{\chi^{-1} + \chi}{2}\cos\alpha\right)P_{n-k-2p}\left(\frac{\chi^{-1} - \chi}{2i}\cos\alpha\right) \times C_{2p}^p\frac{i^{n-k}(-1)^p\chi^{2p}}{2^{2p}}, \tag{35}$$

$$\chi = \sqrt{\frac{\xi_2}{\xi_1}} = \exp\left\{-\frac{TE}{2}\left(\frac{1}{T_2} - \frac{1}{T_1}\right)\right\} \tag{36}$$

(we take into account that $P_{2r+1}(0) = 0$ and $P_{2r}(0) = (-1)^r C_{2r}^r/2^{2r}$, $r = 0, 1, \ldots$; $C_p^q = p!/(q!(p-q)!)$ is the binomial coefficient). A special case $T_1 = T_2$ ($\chi = 1$) (Eq. (30)) can easily be derived from the general case.

Thus, the echo amplitudes can be expressed in terms of the well-known Legendre polynomials, which are built in scientific software. Nevertheless, for the nth echo the number of terms in Eq. (35) increases as n^2. Therefore, Eq. (34) is reasonable to be used if the exact analytical formula for M_n^+ is required. Otherwise, it is much easier to obtain echo amplitudes by straight-forward numerical calculation from the GF, for example, by numerical expansion it in a Taylor series (Eq. (28)) or by Fourier transform (Eq. (29) taking $z = e^{i\vartheta}$); even 1000 and more echoes can be easily calculated by these ways at once. However, for a more clear insight into the behavior of spin echoes it would be preferable to have an approximation and asymptotic form for large echo numbers.

6. Asymptotic behavior of echo-amplitudes in MRI CPMG pulse sequence

6.1. Refocusing angle $\alpha = 0$ or π

If there is no refocusing pulse in the CPMG pulse sequence (the refocusing angle $\alpha = 0$), it is clear that the echo-signal is not formed at all. This exact result also follows immediately from the GF (18). Another exact result can be obtained for $\alpha = \pi$, when T_2 exponential decay of echo-amplitudes takes place, since no longitudinal magnetization is introduced in the transverse plane by π pulse. In this case Eq. (18) can be rewritten in the following form:

$$F(z)|_{\alpha=\pi} = \frac{M_{x0}}{1 - \xi_2 z} + i\frac{M_{y0}}{1 + \xi_2 z} \tag{37}$$

and hence, exact echoes (Eq. (28) or (29)) are

$$M_n^+ = \xi_2^n[M_{x0} + i(-1)^n M_{y0}] \propto \exp\{-nTE/T_2\}. \tag{38}$$

6.2. Refocusing angle $\alpha = \pi/2$, unequal spin relaxation times $T_2 < T_1$

In the CPMG pulse sequence with the refocusing angle $\alpha = \pi/2$ and arbitrary T_1 and T_2 the GF (18) is:

$$\begin{aligned} F(z)|\alpha = \pi/2 &= \frac{M_{x0}}{2}\left[1 + \sqrt{\frac{(1 + \xi_2 z)(1 + \xi_1\xi_2 z^2)}{(1 - \xi_2 z)(1 - \xi_1\xi_2 z^2)}}\right] + i\frac{M_{y0}}{2}\left[1 + \sqrt{\frac{(1 - z\xi_2)(1 - \xi_1\xi_2 z^2)}{(1 + z\xi_2)(1 + \xi_1\xi_2 z^2)}}\right] \\ &= \frac{M_{x0}}{2}\left[1 + \frac{(1 + \xi_2 z)(1 + \xi_1\xi_2 z^2)}{\sqrt{(1 - \xi_2^2 z^2)(1 - \xi_1^2\xi_2^2 z^4)}}\right] + i\frac{M_{y0}}{2}\left[1 + \frac{(1 - \xi_2 z)(1 - \xi_1\xi_2 z^2)}{\sqrt{(1 - \xi_2^2 z^2)(1 - \xi_1^2\xi_2^2 z^4)}}\right]. \end{aligned} \tag{39}$$

Using the following expansion of the radical in Eq. (39):

$$\frac{1}{\sqrt{(1 - \xi_2^2 z^2)(1 - \xi_1^2\xi_2^2 z^4)}} = \sum_{k,m=0}^{\infty} P_{2k}(0)P_{2m}(0) \times (i\xi_2 z)^{2k}(i\xi_1\xi_2 z^2)^{2m}, \tag{40}$$

the exact expression for echoes can be found in a similar way as Eq. (34):

$$\frac{M_{xn}}{M_{x0}} = \frac{(\xi_1\xi_2)^{n/2}}{2}\left(\delta_{n0} + \widetilde{S}_{2[\frac{n}{2}]} + \widetilde{S}_{2[\frac{n-2}{2}]}\right)\left(\cos^2\frac{\pi n}{2} + \chi\sin^2\frac{\pi n}{2}\right),$$
$$\frac{M_{yn}}{M_{y0}} = \frac{(\xi_1\xi_2)^{n/2}}{2}\left(\delta_{n0} + \widetilde{S}_{2[\frac{n}{2}]} - \widetilde{S}_{2[\frac{n-2}{2}]}\right)\left(\cos^2\frac{\pi n}{2} - \chi\sin^2\frac{\pi n}{2}\right), \tag{41}$$

where

$$\widetilde{S}_{2m} = S_{2m}|_{\alpha=\pi/2} = \left(\frac{\chi}{2}\right)^{2m}\sum_{k=0}^{[\frac{m}{2}]}\left(\frac{\chi^2}{2}\right)^{2k} C_{2k}^k C_{2m+4k}^{m+2k}, \tag{42}$$

χ is defined in Eq. (36), $[n]$ is the integral part of n.

For $T_2 < T_1$ the echo-amplitudes asymptotic forms (i.e., for $n \to \infty$) are (see Appendix A):

$$\frac{M_{xn}}{M_{x0}} \approx \frac{(\xi_1\xi_2)^{n/2}}{\sqrt{\pi n(\xi_1-\xi_2)}}\left[\sqrt{\xi_1}\cos^2\frac{\pi n}{2} + \sqrt{\xi_2}\sin^2\frac{\pi n}{2}\right], \tag{43}$$

$$\frac{M_{yn}}{M_{y0}} \approx \frac{(\xi_1\xi_2)^{n/2}}{\sqrt{\pi n(\xi_1+\xi_2)}}\left[\sqrt{\xi_1}\cos\frac{\pi n}{2} - \sqrt{\xi_2}\sin\frac{\pi n}{2}\right]. \tag{44}$$

In this case echo decay is defined by the effective relaxation time $2T_1T_2/(T_1 + T_2)$. It can be explained as follows.

Let us consider one period of the sequence from echo to echo. The refocusing pulse applied along the x axis totally removes the y component of the magnetization vector from the transverse plane and puts the z component into the plane. Therefore, the next echo-signal will be defined only by the x and z magnetization components at the moment of the current echo (for a qualitative explanation we do not consider dephasing of different isochromats). We suppose strict inequality $T_2 < T_1$, so when considering the asymptotic behavior, the contribution from the x component should be neglected, since it relaxes with T_2 for the whole period, while the z one relaxes with T_1 for the first half of the period (from the echo to the pulse) and T_2 for the second half of the period (from the pulse to the echo). Thus, the behavior of echoes with large number is defined by the factor $\sqrt{\xi_1\xi_2}$.

Also note that there is a subdivision between even and odd echoes [17], as shown in Fig. 1. It is also caused by a distinguishing feature of $\pi/2$ pulse consisting in that the longitudinal magnetization returns to the z axis and the y component of the magnetization – to the xy plane in two periods of the pulse sequence. So the relation between consecutive echo amplitudes takes place:

$$\left|\frac{M_{x2k+1}}{M_{x2k}}\right| = \left|\frac{M_{y2k+1}}{M_{y2k}}\right| = \xi_2 = e^{-TE/T_2},$$
$$\left|\frac{M_{x2k+2}}{M_{x2k+1}}\right| \approx \left|\frac{M_{y2k+2}}{M_{y2k+1}}\right| \approx \xi_1 = e^{-TE/T_1} \tag{45}$$

(equality sign in the former equation follows from the exact expressions for echoes (34) and (41)). Thus, the CPMG pulse sequence with $\pi/2$ refocusing angle provides a simple way of simultaneous measurement of T_1 and T_2, while the standard sequence $\alpha = \pi$ allows measurement of T_2 only.

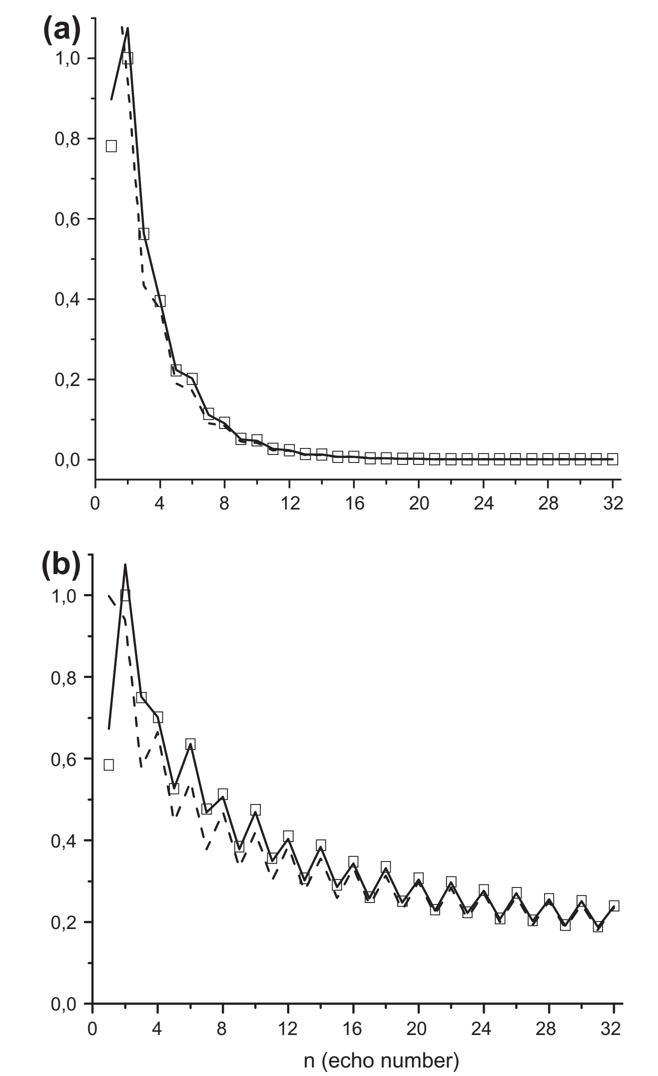

Fig. 1. Exact (open squares), asymptotic (dashed line), and analytically approximated (solid line) echoes (the x component); $\chi = 0.75$, refocusing angle α is $\pi/2$, $T_1 = \infty$ ($\xi_1 = 1$). (a) M_n normalized to the maximum exact echo ($M_{n_{max}}$, $n_{max} = 2$) is shown; (b) value $(\xi_1\xi_2)^{-n/2}M_n$ normalized to the exact value $(\xi_1\xi_2)^{-n_{max}/2}M_{n_{max}}$ is plotted to see better the last echoes.

6.3. Refocusing angle $\alpha \neq 0$, π, equal spin relaxation times $T_1 = T_2$

The case of equal spin relaxation times $T_1 = T_2$ ($\xi_1 = \xi_2 = \xi$) was considered previously in Refs. [12,13], where the following asymptotic forms for echoes were obtained for α in the range $(0, \pi)$ and $n\sin\alpha \gg 1$

$$M_n^+ \approx \xi^n M_{x0}\left[\sin\frac{\alpha}{2} - \frac{\cos\left(n\alpha - \frac{\pi}{4}\right)}{2\sqrt{\pi n^3 \tan\frac{\alpha}{2}}}\right] + i\xi^n M_{y0}\sqrt{\frac{\tan\frac{\alpha}{2}}{\pi n}} \times \cos\left(n\alpha + \frac{\pi}{4}\right). \tag{46}$$

(Note that the expression (46) was obtained in our previous article [13] (Eq. (36)), but the misprint was made: the phase $\pi/4$ in cosine of the imaginary term was missing.) This asymptotic form can be explained as follows. The relaxation just reduces the absolute value of the magnetization (factor ξ^n in Eq. (46)), but does not influence its slope to the xy plane (since $T_1 = T_2$). Therefore, the case $T_1 = T_2 \neq \infty$ differs from the case $T_1 = T_2 = \infty$ by the factor ξ^n only. Thus, to consider the oscillation, we can refer to the case $T_1 = T_2 = \infty$

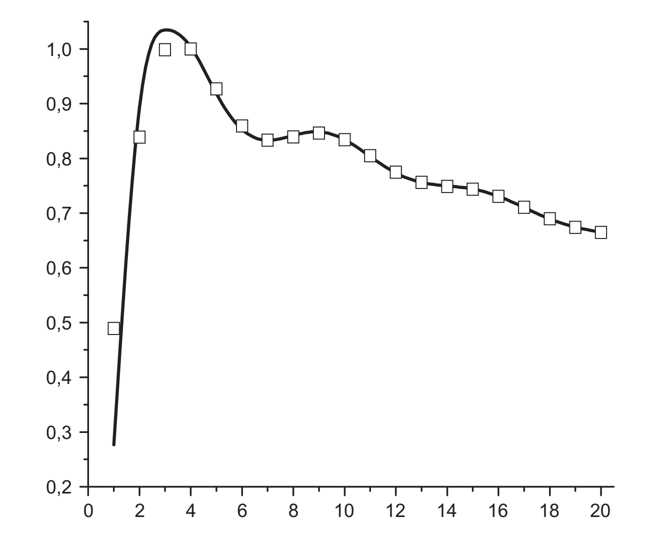

Fig. 2. Exact (open squares) and approximate (solid line) echoes (the x component) normalized to the maximum exact echo ($M_{n_{max}}$, $n_{max} = 4$); $T_1 = T_2$ ($\chi = 1$), refocusing angle α is $\pi/3$, $\xi_1 = \xi_2 = 0.98$.

($\xi = 1$). One can see from Eq. (46) that only M_{xn} includes nonzero stationary value ($M_{xst} = \sin(\alpha/2)$), since RF pulse rotates the magnetization around the x axis, keeping the x component unchanged, while the y and z ones are rotated. It is clear that to perform one complete turn of the magnetization around the x axis, $2\pi/\alpha$ pulses are required, i.e., the period of oscillation is $2\pi/\alpha$ as in Eq. (46) (for a qualitative explanation we do not consider dephasing of different isochromats). Fig. 2 demonstrates the oscillatory behaviour of echoes for $T_1 = T_2$.

Eq. (46) corresponds to the known fact [5], that in absence of spin relaxation the steady state of echoes in the CPMG sequence ($M_{x0} = M_{eq}$, and $M_{y0} = 0$) is $\sin(\alpha/2)$. However, this result was not obtained analytically in Ref. [5] for any α, but followed from numerical solution for the CPMG pulse train. On the contrary, Eq. (46) was derived analytically, using the GF approach.

6.4. Refocusing angle $\alpha \neq 0$, $\pi/2$, π, unequal spin relaxation times $T_2 < T_1$

A more complicated situation takes place for any refocusing angle $\alpha \neq 0, \pi/2, \pi$. For example, it can be shown that for short (but still finite) T_2 the decay of echo-amplitudes occurs with T_1 spin relaxation time instead of T_2.

Indeed, let us consider one period (from echo to echo) of the CPMG sequence of resonant RF pulses with arbitrary refocusing angle $\alpha \neq 0, \pi/2, \pi$. We shall also assume that T_2 is short enough for the transverse magnetization to have died out by the time of the next RF pulse. Then, the next echo-signal will be determined by the longitudinal magnetization turned partially into the xy plane by the pulse, and the behavior of echoes will be governed by the evolution of the z-magnetization. The evolution of the longitudinal component for one period can be described by the factor $\exp(-TE/T_1)\cos\alpha$ (T_1-relaxation and rotation by the RF pulse), and hence, it is likely that the asymptotic behavior will be $M_{x,yn} \propto [\exp(-TE/T_1)\cos\alpha]^n$, i.e., in spite of very short T_2, echo-signal decay can last surprisingly long. This does take place in practice [18,19].

The asymptotic form of echo-amplitudes in the case under consideration is derived in Appendix B and has the form:

$$\frac{M_{xn}}{M_{x0}} \approx A_1 \frac{B^n}{2\sqrt{\pi}} n^{-1/2}, \quad (47)$$

$$\frac{M_{yn}}{M_{y0}} \approx -\frac{B^n}{4A_1\sqrt{\pi}} n^{-3/2}, \quad (48)$$

where

$$A_1 = \sqrt{\frac{(B+\xi_2)(B-\xi_1\cos\alpha)}{(B-\xi_2)\left(B-\frac{1}{2}(\xi_1-\xi_2)\cos\alpha\right)}}, \quad (49)$$

and

$$B = \left(\left|\frac{\xi_1-\xi_2}{2}\cos\alpha\right| + \sqrt{\frac{(\xi_1-\xi_2)^2}{4}\cos^2\alpha + \xi_1\xi_2}\right)\frac{\cos\alpha}{|\cos\alpha|}. \quad (50)$$

From Eqs. (47) and (48) it follows that the asymptotic echo-amplitude decay is not pure exponential, but is determined by the factor B^n and power dependence on n. In particular, if $T_2 \ll T_1$ ($\xi_2 \ll \xi_1$) and $\sqrt{\xi_1/\xi_2}|\cos\alpha| \gg 2$, one obtains $B \approx \exp(-TE/T_1)\cos\alpha$, and the asymptotic behavior corresponds to that discussed above for the case of sufficiently short but finite T_2. Fig. 3 demonstrates a good agreement of exact and asymptotic echoes.

7. Analytical approximation for echoes

In the previous section the asymptotic forms for echo-amplitudes for different cases were considered. However, comparison with the exact results (see the next section) shows that the asymptotic regime can start from very large echo number. In experiment the signal to noise ratio for such echoes with large numbers can be too low. If the analytical formula for echo is required, one can use the exact expression (34). However, it is rather inconvenient, so an acute problem is to find an appropriate approximation that describes adequately the behavior of transient echoes. Below we give such an analytical approximation for echo amplitudes. Derivation of this approximation falls into two cases, whether the parameter χ from Eq. (36) is greater or less than some critical value χ_0:

$$\chi_0 = (1-\sin\alpha)/|\cos\alpha|. \quad (51)$$

These derivations are given in Appendices C and D.

The division between the two cases was made to estimate more accurately the corresponding integrals (see Appendices C and D), while there is no division for the exact echoes (Eq. (34)). This division can be explained as follows. If $T_1 \neq T_2$, the relaxation not only reduces the absolute value of the magnetization, but also changes its slope to the transverse plane, i.e., the magnetization, being turned to the xy plane by the pulse, is returned toward the z axis by the relaxation (compared with what was mentioned in Section 6.3). Thus, the relaxation gives rise to the change of the number of pulses necessary for one complete turn of the magnetization vector around the x axis. Moreover, it can occur that the relaxation does not allow the magnetization make a complete turn around the x axis at all, i.e., at some relation between T_1, T_2, TE and α the

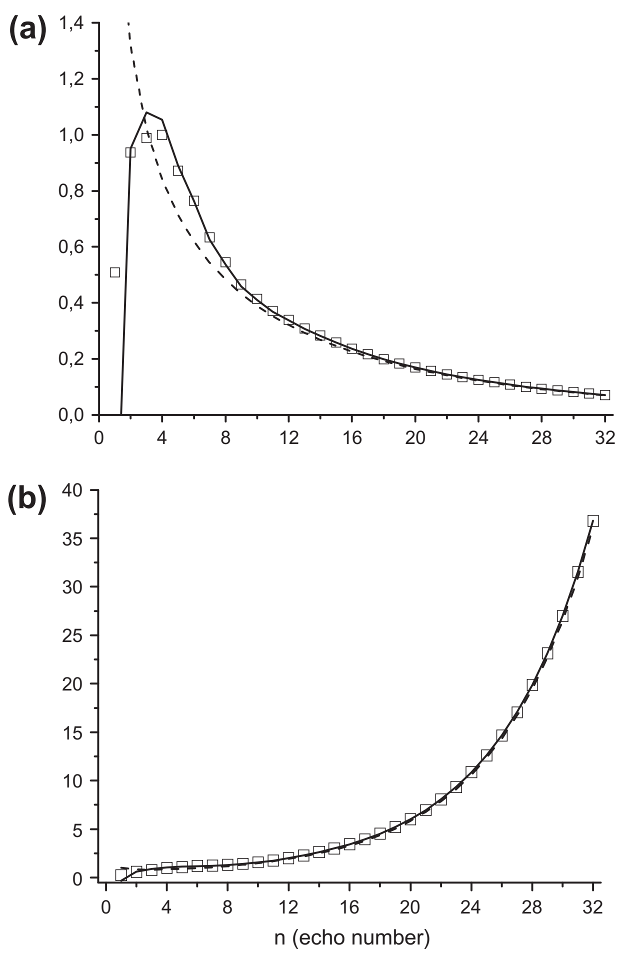

Fig. 3. Exact (open squares), asymptotic (dashed line) and analytically approximated (solid line) echoes (the x component); $\chi = 0.80$, refocusing angle α is $2\pi/9$, $T_1 = \infty$ ($\xi_1 = 1$). (a) M_n normalized to the maximum exact echo ($M_{n_{max}}$, $n_{max} = 4$) is shown; (b) value $(\xi_1\xi_2)^{-n/2}M_n$ normalized to the exact value $(\xi_1\xi_2)^{-n_{max}/2}M_{n_{max}}$ is plotted to see better the last echoes.

oscillation behavior of echoes disappears. For a certain isochromat, this corresponds to the situation when all of the eigenvalues of the Carr–Purcell matrix (the spin evolution matrix in the recursion (9) of Ref. [13]) are real, while in the opposite case there are one real and two complex eigenvalues [9]. When averaging over different isochromats, the transition from the "oscillatory" case to the "non-oscillatory" one is described by the critical value χ_0. From the mathematical point of view, this threshold arises from different arrangement of the singular points of the GF (18) in the complex plane (Figs. 4 and 5).

Strictly speaking, the theoretical limit for the transverse spin relaxation time is $T_2 < 2T_1$ though the condition $T_2 > T_1$ is quite rare

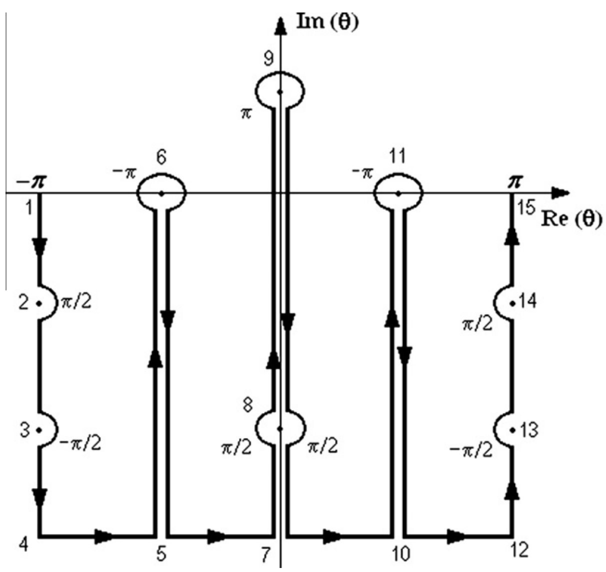

Fig. 4. Integration path in the case cosα > 0 and $\chi_0 < \chi \leqslant 1$. The contour by-passes branch points (the phase changes for the x component are shown near the corresponding branch points).

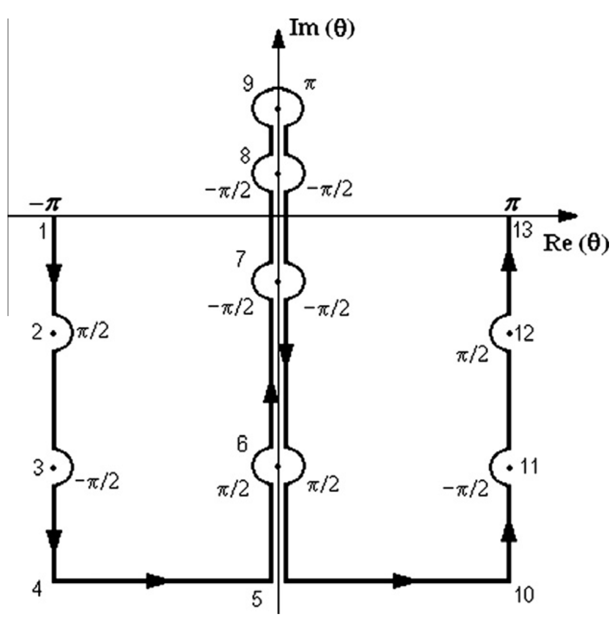

Fig. 5. Integration path in the case cosα > 0 and $\chi \leqslant \chi_0 \leqslant 1$. The contour by-passes branch points (the phase changes for the x component are shown near the corresponding branch points).

in practice [20]. Therefore, in this section we also consider the analytical approximation for $T_2 > T_1$, the derivations are similar to those for $T_2 \leqslant T_1$ described in Appendices C and D. The general condition for the division between the "oscillatory" and "non-oscillatory" cases for any T_1 and T_2 can be specified as follows. For

$$|\ln\chi| < \ln\chi_0^{-1} \tag{52}$$

the analytical approximation includes the oscillations, while in the opposite case

$$|\ln\chi| \geqslant \ln\chi_0^{-1} \tag{53}$$

the oscillations are lacking. Subdivision between the two subcases $T_2 \leqslant T_1$ and $T_2 > T_1$ is cased by the fact, that in the latter subcase the relaxation "presses" the magnetization vector to the *xy* plane, while in the former subcase – to the *z* axis.

Numbers of the equations for the exact, asymptotic and analytically approximated echoes, that are presented in this and previous sections, are summarized in Table 1.

7.1. Case 1: $|\ln\chi| < \ln\chi_0^{-1},\ T_2 \leqslant T_1$

If $|\ln\chi| < \ln\chi_0^{-1}$ ($\alpha \neq 0, \pi$) and $T_2 \leqslant T_1$, the analytical approximation is (see Appendix C):

$$\begin{aligned}\frac{M_{xn}}{M_{x0}} \approx{} & A_1\frac{B^n}{2}p_1^{1/2}\left\{\epsilon I_0\left[\frac{np_1}{2}\right] + (1-\epsilon)I_1\left[\frac{np_1}{2}\right]\right\}e^{-np_1/2} \\ & + A_2\frac{(-\xi_1\xi_2)^n}{4\epsilon B^n}p_2^{1/2}\left\{I_0\left[\frac{np_2}{2}\right] + (2\epsilon-1)I_1\left[\frac{np_2}{2}\right]\right\}e^{-np_2/2} \\ & - A_3\frac{(\xi_1\xi_2)^{n/2}}{2n^{3/2}\sqrt{\pi}}\cos\left(n\beta - \frac{\rho}{2}\right).\end{aligned} \tag{54}$$

Here $I_0[t]$ and $I_1[t]$ are the modified Bessel functions of the 1st kind, and

$$A_2 = \sqrt{\frac{(\xi_1 - B)(B + \xi_2\cos\alpha)}{(\xi_1 + B)\left(B - \frac{1}{2}(\xi_1 - \xi_2)\cos\alpha\right)}}, \tag{55}$$

$$A_3 = \frac{\left(\xi_1\xi_2 - \frac{1}{4}(\xi_1 + \xi_2)^2\cos^2\alpha\right)^{1/4}}{\sqrt{2}(\xi_1\xi_2)^{1/4}\sin\frac{\alpha}{2}}, \tag{56}$$

$$\beta = \arccos\left(\frac{\xi_1 + \xi_2}{2\sqrt{\xi_1\xi_2}}\cos\alpha\right), \tag{57}$$

ρ is the same as in Eq. (C.10) and can be rewritten as:

$$\rho = \arctan\frac{\xi_1\xi_2 + \frac{1}{4}(\xi_1 + \xi_2)^2\cos\alpha}{\frac{1}{2}|\xi_1 - \xi_2|\sqrt{\xi_1\xi_2 - \frac{1}{4}(\xi_1 + \xi_2)^2\cos^2\alpha}} \tag{58}$$

and

$$p_1 = \frac{|B|}{\xi_2} - 1, \tag{59}$$

$$p_2 = \frac{\xi_1}{|B|} - 1, \tag{60}$$

$$\epsilon = \frac{3}{4} + \frac{1}{4}\frac{\cos\alpha}{|\cos\alpha|}. \tag{61}$$

The corresponding expression for the *y* component is:

$$\begin{aligned}\frac{M_{yn}}{M_{y0}} \approx{} & \frac{(-1)^{2\epsilon}B^n}{4A_1 n^{2\epsilon-1}}p_1^{\frac{5}{2}-2\epsilon}\left\{2(1-\epsilon)I_0\left[\frac{np_1}{2}\right] - I_1\left[\frac{np_1}{2}\right]\right\}e^{-np_1/2} \\ & - \frac{(-1)^{2\epsilon}(-\xi_1\xi_2)^n}{4A_2 B^n n^{2-2\epsilon}}p_2^{2\epsilon-\frac{1}{2}}\left\{(2\epsilon-1)I_0\left[\frac{np_2}{2}\right] - I_1\left[\frac{np_2}{2}\right]\right\}e^{-np_2/2} \\ & + \frac{(\xi_1\xi_2)^{n/2}}{A_3\sqrt{\pi n}}\mathrm{Re}\left\{\left(1 - \frac{\kappa}{n}\right)\exp\left[i\left(n\beta + \frac{\rho}{2}\right)\right]\right\},\end{aligned} \tag{62}$$

Table 1
Numbers of the expressions for the exact, asymptotic and analytically approximated echoes (if necessary, in parenthesis the magnetization component is indicated).

Case	Exact expression (apart from Eqs. (28), (29), and (34))	Asymptotic form	Condition for the asymptotic form validity	Analytical approximation
$T_2 \leqslant T_1$ $(\chi \leqslant 1)$				
$\mid \ln \chi \mid < \ln \chi_0^{-1}, \alpha \neq 0, \pi$,				54 (X), 62 (Y)
including				
$T_1 = T_2$	30	46		
$T_2 < T_1$, $\alpha = \pi/2$	41	43 (X), 44 (Y)	65, 68	
$T_2 < T_1$, $\alpha \neq \pi/2$		47 (X), 48 (Y)	65	
$\mid \ln \chi \mid \geqslant \ln \chi_0^{-1}$, $\alpha \neq \pi/2$,				69 (X), 74 (Y)
including				
$\alpha = 0$	No echo			
$\alpha = \pi$	38			
$\alpha \neq 0, \pi$		47 (X), 48 (Y)	75	
$T_2 > T_1$ $(\chi > 1)$				
$\mid \ln \chi \mid < \ln \chi_0^{-1}$, $\alpha \neq 0, \pi$,		85 (X), 87 (Y)	86 (X), 88 (Y)	78 (X), 79 (Y)
including				
$\alpha = \pi/2$	41			
$\mid \ln \chi \mid \geqslant \ln \chi_0^{-1}$, $\alpha \neq \pi/2$		85 (X), 87 (Y)	94 (X), 95 (Y)	89 (X), 90 (Y)

where

$$\kappa = \{(\chi^{-1} - \chi)\cos\alpha\sin\beta[(\chi^{-1} + \chi)\cos\beta - 2] + 2i\left[(\chi^{-1} + \chi)\left(\cos^2\beta - 2\sin^4\frac{\alpha}{2}\right)\cos\beta - 2\right]\} \times \left[8(\chi^{-1} + \chi)\sin^2\alpha\sin\beta\right]^{-1}. \quad (63)$$

The first terms in Eqs. (54) and (62) describe the decay with the factor B, the second ones – with the factor $\xi_1\xi_2/B$, while the third ones describe damped oscillations with a period $2\pi/\beta$. One can see that the period of oscillations in the third terms differs from that for the case $T_1 = T_2$, i.e., $2\pi/\alpha$, and depends also on relation between T_1- and T_2-relaxation, according to what was mentioned above.

For sufficiently short spin–spin relaxation time $T_2 \ll T_1, TE$ one has $\xi_1\xi_2/B \approx \xi_2/\cos\alpha \ll \xi_1\xi_2 \ll B \approx \xi_1\cos\alpha$, so the echo decay occurs with the factor $\xi_1\cos\alpha$, as was discussed above (see Section 6.4).

If $T_1 \neq T_2$ and $\alpha \neq \pi/2$, the first terms in both expressions (54) and (62) dominate at $n \to \infty$, so using the expansion:

$$I_\nu[t] \approx \frac{e^t}{\sqrt{2\pi t}}\left(1 + \frac{1 - 4\nu^2}{8t} + \cdots\right), \qquad t \gg 1, \quad (64)$$

one obtains the corresponding asymptotic expressions (47) and (48). The corresponding condition for the asymptotic form validity is as follows:

$$\frac{n}{2}\left(\frac{|B|}{\xi_2} - 1\right) \gg 1, \quad (65)$$

while the early echoes with the number $n \ll 2(-1 + |B|/\xi_2)^{-1}$ behave like a sum of one or two exponents and damped oscillations:

$$\frac{M_{xn}}{M_{x0}} \approx A_1\frac{\epsilon B^n}{2}p_1^{1/2} + A_2\frac{(-\xi_1\xi_2)^n}{4\epsilon B^n}p_2^{1/2} - A_3\frac{(\xi_1\xi_2)^{n/2}}{2n^{3/2}\sqrt{\pi}} \times \cos\left(n\beta - \frac{\rho}{2}\right), \quad (66)$$

$$\frac{M_{yn}}{M_{y0}} \approx -(1-\epsilon)\frac{B^n}{2A_1}p_1^{3/2} - \left(\epsilon - \frac{1}{2}\right)\frac{(-\xi_1\xi_2)^n}{2A_2B^n}p_2^{3/2} + \frac{(\xi_1\xi_2)^{n/2}}{A_3\sqrt{\pi n}}\mathrm{Re}\left\{\left(1 - \frac{\kappa}{n}\right)\exp\left[i\left(n\beta + \frac{\rho}{2}\right)\right]\right\}. \quad (67)$$

At $T_1 = T_2$ the approximation (54) and the asymptotic form for the x component (Eq. (46)) coincide. Finally, the asymptotic forms (43) and (44) for the special case $\alpha = \pi/2$ (and, hence, $\beta = \pi/2$) can be obtained from the approximation for both $\cos\alpha > 0$ and $\cos\alpha < 0$ tending α to $\pi/2 - 0$ or $\pi/2 + 0$, respectively. From here, the condition for the asymptotic limit validity for $\pi/2$ refocusing angle is:

$$\frac{n}{2}\left(\sqrt{\frac{\xi_1}{\xi_2}} - 1\right) \gg 1. \quad (68)$$

Thus, one can see that the asymptotic form in the case of simultaneous $T_1 = T_2$ and $\alpha = \pi/2$ should be considered as tending T_1 to T_2 (i.e., $\chi \to 1$) first and $\alpha \to \pi/2$ after that, otherwise one obtains the diverging expression (see the discussion in Section 6.2).

7.2. Case 2: $|\ln\chi| \geqslant \ln\chi_0^{-1}$, $T_2 \leqslant T_1$

If $|\ln\chi| \geqslant \ln\chi_0^{-1}$ $(\alpha \neq \pi/2)$ and $T_2 \leqslant T_1$, the analytical approximation is (see Appendix D):

$$\frac{M_{xn}}{M_{x0}} \approx A_1\frac{B^n}{4}p_3^{1/2}\left\{I_0\left[\frac{np_3}{2}\right] + I_1\left[\frac{np_3}{2}\right]\right\}e^{-np_3/2} + A_2\frac{(-\xi_1\xi_2)^n}{4\epsilon B^n}p_2^{1/2}\left\{I_0\left[\frac{np_2}{2}\right] + (2\epsilon - 1)I_1\left[\frac{np_2}{2}\right]\right\}e^{-np_2/2} - A_4\frac{C^n}{4n^{2-2\epsilon}}p_4^{2\epsilon-\frac{1}{2}}\left\{(2\epsilon - 1)I_0\left[\frac{np_4}{2}\right] - I_1\left[\frac{np_4}{2}\right]\right\}e^{-np_4/2}, \quad (69)$$

where

$$A_4 = \sqrt{\frac{(C + \xi_2)\left(\frac{1}{2}(\xi_1 + \xi_2)\cos\alpha - C\right)}{(C - \xi_2)(\xi_1\cos\alpha - C)}}, \quad (70)$$

$$p_3 = \frac{CB}{\xi_1\xi_2} - 1, \quad (71)$$

$$p_4 = \frac{|C|}{\xi_2} - 1, \quad (72)$$

$$C = \left(\frac{\xi_1 + \xi_2}{2}|\cos\alpha| - \sqrt{\frac{(\xi_1 + \xi_2)^2}{4}\cos^2\alpha - \xi_1\xi_2}\right)\frac{\cos\alpha}{|\cos\alpha|}. \quad (73)$$

The corresponding expression for the y component is as follows:

$$\frac{M_{yn}}{M_{y0}} \approx -\frac{B^n}{4A_1}p_3^{3/2}\left\{I_0\left[\frac{np_3}{2}\right] - I_1\left[\frac{np_3}{2}\right]\right\}e^{-np_3/2} - \frac{(-1)^{2\epsilon}(-\xi_1\xi_2)^n}{4A_2B^n n^{2-2\epsilon}}p_2^{2\epsilon-\frac{1}{2}}\left\{(2\epsilon - 1)I_0\left[\frac{np_2}{2}\right] - I_1\left[\frac{np_2}{2}\right]\right\}e^{-np_2/2} + \frac{C^n}{4\epsilon A_4}p_4^{1/2}\left\{I_0\left[\frac{np_4}{2}\right] + (2\epsilon - 1)I_1\left[\frac{np_4}{2}\right]\right\}e^{-np_4/2}. \quad (74)$$

According to the approximations, the echo behavior is described by three terms, which give B-, $\xi_1\xi_2/B$- and C-decay factors, respectively. If $T_2 \ll T_1, TE$, one has $\xi_1\xi_2/B \approx C \approx \xi_2/\cos\alpha \ll B \approx \xi_1\cos\alpha$, and echo amplitude decay occurs with the factor $\xi_1\cos\alpha$, as was discussed above (see Section 6.4).

For $n \to \infty$, $\alpha \neq 0,\pi/2,\pi$ (and, hence, $T_1 \neq T_2$, according to the condition $|\ln\chi| \geqslant \ln\chi_0^{-1}$) the first terms in both expressions (69) and (74) dominate. As in the previous subsection, using the expansion (64), the corresponding asymptotic forms (47) and (48) can be obtained. Thus, the appropriate condition when the asymptotic forms (47) and (48) fit well with the echo amplitudes occurs for:

$$\frac{n}{2}\left(\frac{BC}{\xi_1\xi_2}-1\right) \gg 1, \tag{75}$$

while, again, the early echoes (i.e., $n \ll 2(-1+BC/\xi_1\xi_2)^{-1}$) behave like a sum of from one to three exponents:

$$\frac{M_{xn}}{M_{x0}} \approx A_1\frac{B^n}{4}p_3^{1/2} + A_2\frac{(-\xi_1\xi_2)^n}{4\epsilon B^n}p_2^{1/2} - \left(\epsilon-\frac{1}{2}\right)A_4\frac{C^n}{2}p_4^{3/2}, \tag{76}$$

$$\frac{M_{yn}}{M_{y0}} \approx -\frac{B^n}{4A_1}p_3^{3/2} - \left(\epsilon-\frac{1}{2}\right)\frac{(-\xi_1\xi_2)^n}{2A_2B^n}p_2^{3/2} + \frac{C^n}{4\epsilon A_4}p_4^{1/2}. \tag{77}$$

At $\alpha = 0$ and π the expressions (69) and (74) yield the exact results (see Eq. (38) and the discussion before it).

7.3. Case 3: $|\ln\chi| < \ln\chi_0^{-1}$, $T_2 > T_1$

If $|\ln\chi| < \ln\chi_0^{-1}$ $(\alpha \neq 0,\pi)$ and $T_2 > T_1$, the analytical approximation is:

$$\begin{aligned}\frac{M_{xn}}{M_{x0}} \approx\ & \widetilde{A}_1\frac{\xi_2^n}{2}p_5^{1/2}I_0\left[\frac{np_5}{2}\right]e^{-np_5/2} \\ & - \widetilde{A}_2\frac{(-\xi_2)^n}{4}p_6^{3/2}\left\{I_0\left[\frac{np_6}{2}\right]-I_1\left[\frac{np_6}{2}\right]\right\}e^{-np_6/2} \\ & - A_3\frac{(\xi_1\xi_2)^{n/2}}{2n^{3/2}\sqrt{\pi}}\cos\left(n\beta-\frac{\pi-\rho}{2}\right),\end{aligned} \tag{78}$$

and

$$\begin{aligned}\frac{M_{yn}}{M_{y0}} \approx\ & -\frac{\xi_2^n}{4\widetilde{A}_1 n}p_5^{1/2}I_1\left[\frac{np_5}{2}\right]e^{-np_5/2} \\ & + \frac{(-\xi_2)^n}{4\widetilde{A}_2}p_6^{1/2}\left\{I_0\left[\frac{np_6}{2}\right]+I_1\left[\frac{np_6}{2}\right]\right\}e^{-np_6/2} \\ & + \frac{(\xi_1\xi_2)^{n/2}}{A_3\sqrt{\pi n}}\mathrm{Re}\left\{\left(1-\frac{\kappa}{n}\right)\exp\left[i\left(n\beta+\frac{\pi-\rho}{2}\right)\right]\right\}.\end{aligned} \tag{79}$$

Here

$$\widetilde{A}_1 = \sqrt{\frac{\xi_2+\xi_1}{\xi_2-\xi_1}\cdot 2\tan^2\frac{\alpha}{2}}, \tag{80}$$

$$\widetilde{A}_2 = \sqrt{\frac{\xi_2+\xi_1}{\xi_2-\xi_1}\cdot\frac{1}{2}\cot^2\frac{\alpha}{2}}, \tag{81}$$

$$p_5 = \frac{\widetilde{B}}{\xi_1}-1, \tag{82}$$

$$p_6 = \frac{\xi_2}{\widetilde{B}}-1, \tag{83}$$

$$\widetilde{B} = \left|\frac{\xi_1-\xi_2}{2}\right|\cos\alpha + \sqrt{\frac{(\xi_1-\xi_2)^2}{4}\cos^2\alpha+\xi_1\xi_2}, \tag{84}$$

A_3, ρ and κ are the same as in Eqs. (56), (58) and (63), respectively.

One can see that in this case the echo decay is governed mainly by T_2-relaxation, and only the phase is changed in the oscillation term. At $T_2 = T_1$ the two analytical approximations given here and in Section 7.1 coincide. For $T_2 > T_1$ the asymptotic echo behavior is as follows:

$$\frac{M_{xn}}{M_{x0}} \approx \widetilde{A}_1\frac{\xi_2^n}{2\sqrt{\pi}}n^{-1/2} \tag{85}$$

for

$$\frac{n}{2}\left(\frac{\widetilde{B}}{\xi_1}-1\right) \gg 1, \tag{86}$$

and

$$\frac{M_{yn}}{M_{y0}} \approx \frac{(-\xi_2)^n}{2\widetilde{A}_2\sqrt{\pi}}n^{-1/2} \tag{87}$$

for

$$\frac{n}{2}\left(\frac{\xi_2}{\widetilde{B}}-1\right) \gg 1. \tag{88}$$

This asymptotic form is also valid at $\alpha = \pi/2$, i.e., there is no more subdivision between odd and even echoes for $T_2 > T_1$. This caused by the fact that contrary to the discussion in Section 6.2 for $T_2 < T_1$, here one should neglect T_1-relaxation of the z component and consider only the x one, which is not rotated by the pulse and relaxes with T_2 during the whole pulse sequence (for a qualitative explanation we do not consider dephasing of different isochromats).

7.4. Case 4: $|\ln\chi| \geqslant \ln\chi_0^{-1}$, $T_2 > T_1$

If $|\ln\chi| \geqslant \ln\chi_0^{-1}$ $(\alpha \neq \pi/2)$ and $T_2 > T_1$, the analytical approximation is:

$$\begin{aligned}\frac{M_{xn}}{M_{x0}} \approx\ & \widetilde{A}_1\frac{\xi_2^n}{4\epsilon}p_7^{1/2}\left\{I_0\left[\frac{np_7}{2}\right]+(2\epsilon-1)I_1\left[\frac{np_7}{2}\right]\right\}e^{-np_7/2} \\ & - \widetilde{A}_2\frac{(-\xi_2)^n}{4n^{2-2\epsilon}}p_8^{2\epsilon-\frac{1}{2}}\left\{(2\epsilon-1)I_0\left[\frac{np_8}{2}\right]-I_1\left[\frac{np_8}{2}\right]\right\}e^{-np_8/2} \\ & - \widetilde{A}_4\frac{C^n}{4}p_3^{3/2}\left\{I_0\left[\frac{np_3}{2}\right]-I_1\left[\frac{np_3}{2}\right]\right\}e^{-np_3/2},\end{aligned} \tag{89}$$

and

$$\begin{aligned}\frac{M_{yn}}{M_{y0}} \approx\ & -\frac{\xi_2^n}{4\widetilde{A}_1 n^{2-2\epsilon}}p_7^{2\epsilon-\frac{1}{2}}\left\{(2\epsilon-1)I_0\left[\frac{np_7}{2}\right]-I_1\left[\frac{np_7}{2}\right]\right\}e^{-np_7/2} \\ & + \frac{(-\xi_2)^n}{4\widetilde{A}_2\epsilon}p_8^{1/2}\left\{I_0\left[\frac{np_8}{2}\right]+(2\epsilon-1)I_1\left[\frac{np_8}{2}\right]\right\}e^{-np_8/2} \\ & + \frac{C^n}{4\widetilde{A}_4}p_3^{1/2}\left\{I_0\left[\frac{np_3}{2}\right]+I_1\left[\frac{np_3}{2}\right]\right\}e^{-np_3/2}.\end{aligned} \tag{90}$$

Here

$$\widetilde{A}_4 = \frac{\cos\alpha}{|\cos\alpha|}\sqrt{\frac{(\xi_2+C)\left(\frac{1}{2}(\xi_1+\xi_2)\cos\alpha-C\right)}{(\xi_2-C)(\xi_2\cos\alpha-C)}}, \tag{91}$$

$$p_7 = 2(1-\epsilon)\frac{\xi_2}{|B|}+(2\epsilon-1)\frac{|C|}{\xi_1}-1, \tag{92}$$

$$p_8 = (2\epsilon-1)\frac{\xi_2}{|B|}+2(1-\epsilon)\frac{|C|}{\xi_1}-1. \tag{93}$$

As in previous case, the echo decay is governed mainly by T_2-relaxation. The corresponding asymptotic form coincides with that given by Eqs. (85) and (87), but the conditions for asymptotic limit validity are different:

$$\frac{n}{2}\left[2(1-\epsilon)\frac{\xi_2}{|B|}+(2\epsilon-1)\frac{|C|}{\xi_1}-1\right] \gg 1 \qquad \texttt{for}\ M_{xn}, \tag{94}$$

$$\frac{n}{2}\left[(2\epsilon-1)\frac{\xi_2}{|B|}+2(1-\epsilon)\frac{|C|}{\xi_1}-1\right] \gg 1 \qquad \texttt{for}\ M_{yn}. \tag{95}$$

At $\alpha = 0$ and π this approximation also yields the exact results (Section 6.1).

8. Analysis of asymptotic form and approximation accuracy

To test the asymptotic forms and analytical approximations obtained, we have made up a table showing an echo number, from which the corresponding expression describes adequately the exact echoes (Tables 2 and 3). As a criterion, the following condition was chosen:

$$\delta = \left| \frac{M_n^{\text{ap}}}{M_n^{\text{ex}}} - 1 \right| \leqslant 0.05 \tag{96}$$

(the superscripts "ap" and "ex" denote the approximated (by the asymptotic form or analytical approximation) echo amplitude and the exact one, respectively). Besides, since the situation $T_2 > T_1$ is quite exotic, the analysis was performed for $T_2 \leqslant T_1$ ($\chi \leqslant 1$) only.

In Tables 2 and 3 the data format $n_1/n_2(n_3)/n_4$ was chosen, that means the following. The numbers n_1 and n_2 are the echo numbers, from which the criterion (96) is fulfilled for the asymptotic form and the approximation, respectively; these numbers are shown if only they less than or equal 100. The number n_3 in parenthesis is the actual echo number from which the analytical approximation can be used with the criterion (96) fulfilled, n_3 is shown if only $n_3 < n_2, n_4$. The appearance of n_3 is caused by the exclusion of some outlying values of δ for very small echoes ($M_n/M_{nmax} \leqslant 0.01$), since the analytical approximation also yields very small values of the same order, but its accuracy is not sufficient for the criterion (96) to be fulfilled. For comparison, the number n_4 is presented, which is the echo number, from which the exact echo damps by 100 times compared with the maximum one; n_4 is shown if only it is less than or equal 100. The boundary between the oscillatory (to the right of the boundary) and non-oscillatory (to the left of the boundary) cases of the analytical approximation is in bold type. Refocusing angles $\alpha = 0$ and π are not presented, since in these cases the exact solutions are possible, and the analytical approximation also reproduces the exact results.

One can see that, as $|\cos\alpha|$ increases, the asymptotic regime starts later (number n_1). It can readily be verified (Eq. (34)) that echo amplitudes can be represented as:

$$M_n(\xi_1, \xi_2, \alpha) = (\xi_1 \xi_2)^{n/2} \widetilde{M}_n(\chi, \alpha) = \xi_1^n \chi^n \widetilde{M}_n(\chi, \alpha). \tag{97}$$

Thus, for example, for low α and χ the asymptotic form starts working well too late, when the echo signal level can be rather low. At fixed α, with decreasing χ the asymptotic form first begins working earlier, and then with further decrease in χ – later. The best point for the asymptotic form lies near the boundary between the oscillatory and non-oscillatory cases. This corresponds to the conditions for the validity of the asymptotic forms (Eqs. (65) and (75)): if $\chi_0 < \chi \leqslant 1$, the asymptotic threshold $n_{as} = 2(b\chi^{-1} - 1)^{-1}$ (b is defined in Eq. (C.12)) decreases with decreasing χ, while for $\chi \leqslant \chi_0 \leqslant 1$ the corresponding asymptotic threshold $n_{as} = 2(bc - 1)^{-1}$ (c is defined in Eq. (D.5)) increases with decreasing χ.

As for analytical approximation, it starts working much earlier (numbers n_2 and n_3 in Tables 2 and 3) than the asymptotic form (number n_1 in the tables). The approximation for M_{yn} is worse than that for M_{xn}. This is caused by the features of the integrals to be estimated. Near the point $\chi = \chi_0$ the analytical approximation becomes worse, but still good enough. In this region the estimation of the corresponding integrals (see Appendices C and D) can be carried out similarly, but this special case is not treated in the present work not to complicate the consideration.

The error of the approximate equations are also caused by the following fact. When the corresponding integrals were estimated (see Appendices C and D), only closeness of two out of all singular points of the GF was taken into account (points 8 and 9, 13 and 14 in Fig. 4; and points 6 and 7, 8 and 9, 11 and 12 in Fig. 5). However, for instance, near the boundary between oscillatory and non-oscillatory cases, points 6 and 11 in Fig. 4 and 7 and 8 in Fig. 5 come close, and this should be also taken into account for higher accuracy, while we neglected this effect. Also, in the region of simultaneous tending $\chi \to 1$ ($T_2 \to T_1$) and $|\cos\alpha| \to 1$ the closeness of more singular points should be considered, viz. points 6, 8, 9 and 11 in Fig. 4 and points 6, 7, 8 and 9 in Fig. 5. The next corrections to the estimation can be calculated, but the form of the equations becomes more complicated. We suppose, if one is interested in an accurate analytical formula for the first echoes, the exact expression (34) can be used. However, echoes can be easily calculated numerically from the GF at once, for example, by numerical expansion it in a Taylor series (Eq. (28)) or by Fourier transform of the GF [12,13].

Figs. 1–3 demonstrate good agreement between approximated and exact echoes in the region, where it is sufficient to take into account the correlation between two of the singular points only.

Table 2
The accuracy of the asymptotic forms and analytical approximations for different values $\chi = \sqrt{\xi_2/\xi_1}$ and α in terms of n_1, n_2, n_3 and n_4; the x component (at $\chi = 1$, i.e., $T_1 = T_2$, the asymptotic form and analytical approximation coincide).

α (°)	χ									
	0.1	0.2	0.3	0.4	0.5	0.6	0.7	0.8	0.9	1
10	–/1/–	–/1/–	–/1/–	–/1/–	–/1/–	–/1/–	–/1/–	**72/1**/–	**14/27**/–	16/16/–
20	–/1/77	–/1/79	–/1/84	–/1/92	78/1/–	48/1/–	**25/12**/–	**7/12**/–	22/9/–	8/8/–
30	–/2/34	–/2/36	94/2/38	51/2/40	**29/2/48**	**15/18/58**	5/8/75	12/6/–	31/6/–	6/6/–
40	–/2/20	–/2/21	44/2/32	**23/2/24**	**11/13/28**	4/5/34	9/4/44	16/5/63	34/5/–	5/5/–
50	–/2/13	50/2/13	**21/4/14**	**9/11/16**	4/2/19	7/2/23	8/4/29	15/4/43	36/4/82	4/4/–
60	96/2/9	**23/4/9**	**8/9/10**	3/2/12	6/2/14	7/3/17	12/3/22	18/4/32	41/4/62	3/3/–
70	**38/2/7**	**8/9/7**	5/2/8	5/2/9	5/2/11	9/3/13	15/3/17	21/3/25	45/3/49	3/3/–
80	**8/8/5**	5/2/6	6/2/6	9/4/7	9/4/9	13/3/11	21/3/14	27/3/21	57/3/41	3/3/–
90	**16/8(2)/3**	20/4/5	20/4/5	20/6/7	20/6/7	24/3/9	28/3/18	36/3/18	64/3/35	1/1/–
100	**9/9/5**	6/4/5	10/4/5	12/6(5)/7	20/8(4)/5	28/12(4)/7	42/18(3)/11	74/34(3)/17	–/90(2)/32	2/2/–
110	**39/2/6**	**10/10/7**	6/4/7	8/4/7	12/6/8	16/8(6)/9	24/12(2)/11	41/20(2)/15	96/50(2)/29	2/2/–
120	96/1/8	**25/5/8**	**12/11/9**	8/6/9	8/6/10	12/6(4)/11	18/8(2)/12	30/16(2)/16	72/38(2)/29	2/2/–
130	–/2/11	51/1/11	**23/6/11**	**14/12/11**	10/8/12	10/6/13	16/8(2)/13	26/12(2)/17	58/31(2)/29	2/2/–
140	–/2/14	–/1/14	46/1/15	**26/8/15**	**17/15/15**	14/10/17	14/8/17	24/12(2)/18	52/2/29	2/2/–
150	–/1/20	–/1/20	96/1/21	54/1/21	**34/8/21**	**24/20/21**	18/12/21	24/12(2)/19	50/28(2)/27	2/2/–
160	–/1/30	–/1/31	–/1/31	–/1/30	83/1/28	55/6(1)/26	**38/23(7)/22**	**28/18(10)/17**	50/30(2)/27	2/2/–
170	–/1/28	–/1/25	–/1/19	–/1/11	–/1/7	–/1/7	–/1/9	**91/18(1)/13**	**60/38(2)/25**	2/2/–

Table 3
The accuracy of the asymptotic forms and analytical approximations for different values $\chi = \sqrt{\xi_2/\xi_1}$ and α in terms of n_1, n_2, n_3 and n_4; the y component.

α (°)	χ									
	0.1	0.2	0.3	0.4	0.5	0.6	0.7	0.8	0.9	1
10	–/1/–	–/1/–	–/1/–	–/1/–	–/1/–	–/1/–	–/2/–	–/**2**/–	**64**/**86**/–	–/23 (6)/–
20	–/1/76	–/1/73	–/1/70	–/1/66	–/3/62	–/7/59	**73**/**37**/**55**	**33**/**41**/**48**	78/37(2)/47	–/3/–
30	–/2/34	–/1/33	–/1/31	–/8/29	**82**/**7**/**28**	**43**/**52**/**26**	23/26/25	40/10/22	99/50(2)/31	56/3/–
40	–/2/9	–/2/19	–/8/18	**64**/**6**/**17**	**32**/**38**/**16**	18/17/15	22/11(3)/16	48/7(2)/16	–/62(2)/32	–/2/–
50	–/2/13	–/8/12	**59**/**6**/**12**	**27**/**31**/**11**	15/12/9	18/7(3)/11	32/6/12	60/2/19	–/94(2)/33	99/2/–
60	–/2/9	**66**/**6**/**9**	**25**/**27**/**8**	13/10/7	18/3/7	27/12(5)/10	50/8(5)/10	86/38(1)/16	–/–(1)/30	26/2/–
70	–/**8**/**7**	**24**/**25**/**6**	12/8(3)/5	19/5/6	29/5/8	49/27(1)/9	74/43(7)/11	–/83(1)/16	–/12(1)/31	71/1/–
80	**24**/**25**/**5**	28/2/4	31/4/6	44/16(4)/6	70/34(3)/8	–/65(3)/10	–/63(2)/12	–/40(1)/16	–/1/32	60/1/–
90	**20**/**4**(**2**)/**3**	20/4/5	20/4/5	20/3/7	20/3/7	20/3/9	24/2/11	29/1/16	45/1/28	5/1/–
100	**27**/**26**/**5**	16/5/5	29/16(2)/4	42/21(2)/6	64/34(3)/8	91/14(3)/9	–/14(3)/11	–/32(5)/17	–/86(7)/31	50/1/–
110	–/**7**/**6**	**30**/**28**/**6**	19/14/6	22/13/5	32/13(6)/7	42/23(3)/9	67/33(3)/10	98/54(8)/15	–/44(8)/30	44/3/–
120	8/2/8	**70**/**23**/**8**	**34**/**32**/**8**	24/19/7	25/15/6	31/15(7)/10	43/20(3)/11	72/38(7)/17	–/86(3)/29	15/1/–
130	–/2/11	–/6/10	**67**/**26**/**10**	**41**/**37**/**10**	31/24/9	30/18/8	37/18(11)/13	58/24(8)/14	–/60(8)/28	47/1/–
140	–/2/14	–/2/14	–/4/14	**75**/**31**/**13**	**51**/**46**/**13**	41/30/12	39/22/15	54/22(4)/17	–/48(9)/34	54/1/–
150	–/1/20	–/1/20	–/1/20	–/1/20	**99**/**38**/**19**	**70**/**31**/**18**	56/40/18	54/28/23	96/40(13)/34	18/1/–
160	–/1/31	–/1/31	–/1/31	–/1/31	–/1/31	–/48/30	–/**74**/**29**	**86**/**58**/**30**	93/41(25)/35	89/8/–
170	–/1/30	–/1/33	–/1/38	–/1/44	–/1/50	–/1/55	–/7/58	–/**98**/**59**	–/–/**61**	–/15/–

9. Conclusions

Employing the generating functions formalism [12,13], exact explicit analytical expression for echoes in the Carr–Purcell–Meiboom–Gill sequence with arbitrary excitation and refocusing angles and resonance offset of RF pulses was obtained. It was shown, that the exact echo amplitudes can be expressed in terms of Legendre polynomials.

Asymptotic form for echoes was derived in an elegant way and analyzed in details. It was shown that the following cases for the asymptotic regime can be distinguished. The first one is the case of refocusing angle $\alpha = 0$ or π, when the well-known exact solutions exist (no echo at $\alpha = 0$ and the result (38) at $\alpha = \pi$). The second one is the case $\alpha = \pi/2$ and $T_1 \neq T_2$, when the echo behavior is defined not only by T_1 or T_2, but by the effective relaxation time $2T_1T_2/(T_1 + T_2)$; besides, a subdivision between even and odd echoes is observed. The third case is $\alpha \neq 0, \pi$ and $T_1 = T_2$, when damped oscillations with a period $2\pi/\alpha$ are to manifest themselves. And the last case is $\alpha \neq 0, \pi/2, \pi$ and $T_1 \neq T_2$, when, for example, at sufficiently rapid spin–spin relaxation the echo amplitude decay is defined by T_1 and refocusing angle α, rather than by T_2.

However, for some parameter sets the asymptotic form starts to adequately describe the echo behavior very late, when experimental signal level can be too low. To improve the description, we obtained the analytical approximation that corresponds to the exact echoes starting from sufficiently small echo number. This approximation derived from the GF is convenient for numerical and analytical analysis, since it does not contain any multiple sums, but only well-known analytical functions (the 0th- and 1st-order modified Bessel functions of the 1st kind). It was shown that, depending on the relationship of parameters $\cos\alpha$ and ξ_2/ξ_1, the echo behavior can be described by three terms containing either three pseudo-exponential decays or two pseudo-exponential decays and damped oscillations. Numerical comparison shows good agreement between approximate and exact echoes.

Besides, it was shown that the generating function approach can also be applied to the consideration of terminated pulse sequences, when after-pulses echoes are registered. The nonnull-configurations of the generating function for a definite isochromat, which are actually the generating functions for after-pulses echo amplitudes, were determined.

Acknowledgments

This work was supported by Russian Foundation for Basic Research (RFBR) (Grant No. 11-03-00296), President grant for supporting the Leading Scientific Schools (7643.2010.3) and the Division of Chemistry and Material Science of the RAS grant (No. 5.1.1.).

Appendix A. Derivation of Eq. (43)

Let us consider the CPMG pulse sequence with the refocusing angle $\alpha = \pi/2$. The corresponding GF for echo-amplitudes takes the form (39). Let us introduce a new variable $y = z\sqrt{\xi_1\xi_2}$, so Eq. (39) can be rewritten as

$$F(y) = \frac{M_{x0}}{2}\left[1 + \sqrt{\frac{(1+\chi y)(1+y^2)}{(1-\chi y)(1-y^2)}}\right] + i\frac{M_{y0}}{2}\left[1 + \sqrt{\frac{(1-\chi y)(1-y^2)}{(1+\chi y)(1+y^2)}}\right], \quad \text{(A.1)}$$

where χ is the same as in Eq. (36), $\chi < 1$ for $T_2 < T_1$. We will consider the x component only, as the y-one can be treated similarly. Then, according to the complex function theory, M_{xn} ($n \geqslant 1$) can be calculated by the contour integral:

$$\frac{M_{xn}}{M_{x0}} = \frac{1}{2}\frac{(\xi_1\xi_2)^{n/2}}{2\pi i}\oint\sqrt{\frac{(1+\chi y)(1+y^2)}{(1-\chi y)(1-y^2)}}\frac{dy}{y^{n+1}}. \quad \text{(A.2)}$$

The zeros of the numerator and denominator of the radical in Eq. (A.2) are $\pm\chi^{-1}$, $\pm i$, ± 1. Taking $y = e^{i\theta}$, the contour of integration contains four singular points, and the expression (A.2) can be rewritten as:

$$\begin{aligned}\frac{M_{xn}}{M_{x0}} &= \frac{(\xi_1\xi_2)^{n/2}}{2\pi}\mathrm{Re}\int_0^{\pi}\left[\frac{(1+\chi e^{i\theta})(1+e^{2i\theta})}{(1-\chi e^{i\theta})(1-e^{2i\theta})}\right]^{1/2} e^{-in\theta}\,d\theta \\ &= \frac{(\xi_1\xi_2)^{n/2}}{2\pi}\mathrm{Re}\left\{e^{i\pi/4}\int_0^{\pi/2}\left[\frac{\cos\theta}{\sin\theta}\,\frac{(1+\chi e^{i\theta})}{(1-\chi e^{i\theta})}\right]^{1/2} e^{-in\theta}\,d\theta\right. \\ &\left. + e^{-i\pi/4}\int_{\pi/2}^{\pi}\left[-\frac{\cos\theta}{\sin\theta}\,\frac{(1+\chi e^{i\theta})}{(1-\chi e^{i\theta})}\right]^{1/2} e^{-in\theta}\,d\theta\right\}. \quad \text{(A.3)}\end{aligned}$$

In the second integral it was taken into account that, when passing the point $\theta = \pi/2$ ($y = i$), the phase changed to $e^{-i\pi/2}$. Making the change of variable $\theta = \pi - x$ ($\theta \to \pi - \theta$) in the second integral, one obtains

$$\frac{M_{xn}}{M_{x0}} = \frac{(\xi_1\xi_2)^{n/2}}{2\pi}\mathrm{Re}\left\{e^{i\pi/4}\int_0^{\pi/2}\left[\frac{\cos\theta(1+\chi e^{i\theta})}{\sin\theta(1-\chi e^{i\theta})}\right]^{1/2}e^{-in\theta}\,d\theta + e^{-i\pi/4-in\pi}\int_0^{\pi/2}\left[\frac{\cos\theta(1-\chi e^{i\theta})}{\sin\theta(1+\chi e^{i\theta})}\right]^{1/2}e^{in\theta}\,d\theta\right\}. \tag{A.4}$$

When $n \to \infty$, the main contribution to the integrals is determined by $\theta \to 0$ ($\cot\theta \to 1/\theta$), i.e.,

$$\frac{M_{xn}}{M_{x0}} \approx \frac{(\xi_1\xi_2)^{n/2}}{2\pi}\left[\sqrt{\frac{1+\chi}{1-\chi}} + \sqrt{\frac{1-\chi}{1+\chi}}\cos n\pi\right] \times \int_0^{\pi/2}\frac{\cos(n\theta-\pi/4)}{\sqrt{\theta}}\,d\theta. \tag{A.5}$$

Again, making the change $\theta \to n\theta$ and using

$$\int_0^\infty \frac{\sin x}{\sqrt{x}}\,dx = \int_0^\infty \frac{\cos x}{\sqrt{x}}\,dx = \sqrt{\frac{\pi}{2}} \tag{A.6}$$

one obtains the result (43). The expression (43) diverges for $\xi_1 \to \xi_2$, so the generate case $\xi_1 = \xi_2$ should be considered separately, and the condition $n(\chi^{-1}-1)/2 \gg 1$ for the asymptotic form (43) can be written.

Appendix B. Derivation of Eq. (47)

Consider now the case of refocusing angle $\alpha \neq \pi/2, \pi$ and unequal spin relaxation times $T_1 > T_2$ ($\xi_1 > \xi_2$). Introducing $y = z\sqrt{\xi_1\xi_2}$, one can rewrite the GF (18) as:

$$F(y) = \frac{M_{x0}}{2}\left[1+\sqrt{\frac{X(y)}{Y(y)}}\right] + i\frac{M_{y0}}{2}\left[1+\sqrt{\frac{Y(y)}{X(y)}}\right],$$
$$X(y) = (1+y\chi)\left[1-y(\chi^{-1}+\chi)\cos\alpha+y^2\right], \tag{B.1}$$
$$Y(y) = (1-y\chi)\left[1-y(\chi^{-1}-\chi)\cos\alpha-y^2\right]$$

and

$$M_n^+ = \frac{(\xi_1\xi_2)^{n/2}}{2\pi i}\oint F(y)\frac{dy}{y^{n+1}}. \tag{B.2}$$

We will consider the x component of the magnetization only, as the y one can be considered in a similar way.

First we assume that $0 < \alpha < \pi/2$ ($\cos\alpha > 0$), then, in addition to singular points $\pm 1/\chi$ outside the unit circle, four more singular points exist:

$$y_1 = \frac{\chi^{-1}+\chi}{2}\cos\alpha + \sqrt{\frac{1}{4}(\chi^{-1}+\chi)^2\cos^2\alpha - 1},$$
$$y_2 = \frac{\chi^{-1}+\chi}{2}\cos\alpha - \sqrt{\frac{1}{4}(\chi^{-1}+\chi)^2\cos^2\alpha - 1},$$
$$y_3 = -\frac{\chi^{-1}-\chi}{2}\cos\alpha + \sqrt{\frac{1}{4}(\chi^{-1}-\chi)^2\cos^2\alpha + 1}, \tag{B.3}$$
$$y_4 = -\frac{\chi^{-1}-\chi}{2}\cos\alpha - \sqrt{\frac{1}{4}(\chi^{-1}-\chi)^2\cos^2\alpha + 1}.$$

The point $y_4 < -1$ lies outside, and the point $0 < y_3 < 1$ – inside the unit circle. The positions of y_1 and y_2 depend on $x = \frac{1}{2}(\chi^{-1}+\chi)\cos\alpha$: if $x \leqslant 1$, then y_1 and y_2 lie on the unit circle ($|y_1| = |y_2| = 1$), otherwise, $y_1 > 1$ and $0 < y_2 < 1$. It is easy to show that $|y_3| < |y_2|$ for any x. Indeed, the statement is obvious for $x \leqslant 1$, and for $x > 1$ the desired inequality can be represented in the following form:

$$\sqrt{x^2+p} - \sqrt{x^2-1+p} < x - \sqrt{x^2-1}, \tag{B.4}$$

where $p = \sin^2\alpha$. At $p = 0$ ($\alpha = 0$) the two sides of the inequality (B.4) are equal, but this case corresponds to the absence of echo-signal and is out of interest. For any $p > 0$ the derivative of the left-hand side of the inequality (B.4) with respect to p is

$$\frac{1}{2\sqrt{x^2+p}} - \frac{1}{2\sqrt{x^2-1+p}} < 0, \tag{B.5}$$

and thus, the left-hand side of Eq. (B.4) decreases with increasing p, i.e., $y_3 < y_2$. Thus, assuming $y = y_3\,e^{i\theta}$ for any x, one obtains:

$$\frac{M_{xn}}{M_{x0}} = \mathrm{Re}\left\{\int_0^\pi\left[\frac{(1+\chi y_3e^{i\theta})(y_3e^{i\theta}-y_1)(y_3e^{i\theta}-y_2)}{(1-\chi y_3e^{i\theta})(y_3e^{i\theta}-y_4)y_3(1-e^{i\theta})}\right]^{1/2} \times \frac{(\xi_1\xi_2)^{n/2}}{2\pi y_3^n}e^{-in\theta}\,d\theta\right\}. \tag{B.6}$$

For $n \to \infty$ the main contribution to the integral is determined by $\theta \to 0$, and therefore,

$$\frac{M_{xn}}{M_{x0}} \approx \frac{(\xi_1\xi_2)^{n/2}}{2\pi y_3^n}\left[\frac{(1+\chi y_3)(y_3-y_1)(y_3-y_2)}{2(1-\chi y_3)(y_3-y_4)y_3}\right]^{1/2} \times \int_0^\pi\frac{\cos\left(n\theta-\frac{\pi}{4}\right)}{\sqrt{\theta}}d\theta = \frac{B^n}{2\sqrt{\pi n}}\sqrt{\frac{(B+\xi_2)(B-\xi_1\cos\alpha)}{(B-\xi_2)(B-1/2(\xi_1-\xi_2)\cos\alpha)}}. \tag{B.7}$$

Considering the case $\pi/2 < \alpha < \pi$ ($\cos\alpha < 0$) in a similar way, one obtains Eq. (47).

Appendix C. Derivation of the analytical approximation (54)

If $(1-\sin\alpha)/|\cos\alpha| < \chi \leqslant 1$ and $0 < \alpha < \pi$, not all the roots (B.3) are real, viz. y_1 and y_2 lie on the unity circle. We first assume that $\cos\alpha \geqslant 0$, since the case $\cos\alpha < 0$ can be considered in a similar way. Taking $y = e^{i\theta}$ in Eq. (B.2), one obtains:

$$\frac{M_n^+}{(\xi_1\xi_2)^{n/2}} = \frac{1}{4\pi}\int_{-\pi}^{\pi}\left(M_{x0}\sqrt{\frac{X(e^{i\theta})}{Y(e^{i\theta})}} + iM_{y0}\sqrt{\frac{Y(e^{i\theta})}{X(e^{i\theta})}}\right)e^{-in\theta}\,d\theta. \tag{C.1}$$

Let us change the integration path to that shown in Fig. 4. When bypassing the branch points, the radical phase changes should be taken into account, as shown in the same figure (we will treat the x component only, since the y one can be treated in a similar way). Taking into account the direction of integration as well, it can readily be verified that only the following integrals contribute to the integral in Eq. (C.1):

$$\int_{-\pi}^{\pi} = 2\left\{\int_9^8 - \int_{14}^{13} + \left(\int_{11}^{10} - \int_6^5\right)\right\} \tag{C.2}$$

(the indices denote the direction of integration, all integrals mean principal values). Let us denote $y_1 = e^{i\beta}$ and $\beta = \arccos\left(\frac{1}{2}(\chi^{-1}+\chi)\cos\alpha\right)$ and consider each of the integrals separately (in what follows $I_k[t]$ means the modified Bessel function of the 1st kind).

C.1. Integration from the point 9 to the point 8

Taking $\theta = -i\ln y_3 - it$, the integral $\int_9^8$ can be rewritten as follows:

$$\int_9^8\sqrt{\frac{X}{Y}}e^{-in\theta}\,d\theta = -\frac{ie^{i\pi/2}}{y_3^n} \times \int_0^{-\ln(\chi y_3)}\sqrt{\frac{(1+\chi y_3e^t)(y_3e^t-y_1)(y_3e^t-y_2)}{(1-\chi y_3e^t)y_3(e^t-1)(y_3e^t-y_4)}}e^{-nt}dt. \tag{C.3}$$

For $n \gg 1$ the integral (C.3) can be estimated as

$$\int_9^8 \sqrt{\frac{X}{Y}} e^{-in\theta} d\theta \approx \frac{1}{y_3^n} \sqrt{\frac{(\chi^{-1}+y_3)(y_3-y_1)(y_3-y_2)}{y_3^2(y_3-y_4)}} \times \int_0^{-y_4\chi^{-1}-1} \frac{e^{-nt}}{t^{1/2}(-y_4\chi^{-1}-1-t)^{1/2}} dt = \frac{\pi}{y_3^n} \times \sqrt{\frac{(\chi^{-1}+y_3)(y_3-y_4-2\cos\beta)}{1+y_3^2}} I_0\left[-n\frac{\chi+y_4}{2\chi}\right] \exp\left[n\frac{\chi+y_4}{2\chi}\right]. \quad (C.4)$$

C.2. Integration from the point 14 to the point 13

Taking $\theta = \pi - i\ln(-y_4) - it = \pi + i\ln y_3 - it$, the integral $\int_{14}^{13}$ can be rewritten as follows:

$$\int_{14}^{13} \sqrt{\frac{X}{Y}} e^{-in\theta} d\theta = -\frac{ie^{-i\pi/2}}{y_4^n} \times \int_0^{\ln(y_3/\chi)} \sqrt{\frac{(-1-\chi y_4 e^t)(y_4 e^t - y_1)(y_4 e^t - y_2)}{(1-\chi y_4 e^t) y_4 (e^t-1)(y_3 - y_4 e^t)}} e^{-nt} dt. \quad (C.5)$$

For $n \gg 1$ the integral (C.5) can be estimated as

$$\int_{14}^{13} \sqrt{\frac{X}{Y}} e^{-in\theta} d\theta \approx -\frac{1}{y_4^n} \sqrt{\frac{(y_4-y_1)(y_4-y_2)}{(\chi^{-1}-y_4)(y_3-y_4)}} \times \int_0^{y_3\chi^{-1}-1} \frac{(y_3\chi^{-1}-1-t)^{1/2}}{t^{1/2}} e^{-nt} dt = -\frac{\pi}{y_4^n} \frac{y_3-\chi}{2\chi} \sqrt{\frac{(y_4-y_1)(y_4-y_2)}{(\chi^{-1}-y_4)(y_3-y_4)}} \times \left\{ I_0\left[n\frac{y_3-\chi}{2\chi}\right] + I_1\left[n\frac{y_3-\chi}{2\chi}\right] \right\} \exp\left[-n\frac{y_3-\chi}{2\chi}\right]. \quad (C.6)$$

C.3. Integration from the point 11 to the point 10 and from 6 to 5

Taking $\theta = \beta - it$, the integral $\int_{11}^{10}$ can be rewritten as follows:

$$\int_{11}^{10} \sqrt{\frac{X}{Y}} e^{-in\theta} d\theta = -ie^{-in\beta} \times \int_0^\infty \sqrt{\frac{(1+\chi e^{i\beta}e^t)e^{i\beta}(e^t-1)(e^{i\beta}e^t - e^{-i\beta})}{(\chi e^{i\beta}e^t - 1)(e^{i\beta}e^t - y_3)(e^{i\beta}e^t - y_4)}} e^{-nt} dt. \quad (C.7)$$

For $n \gg 1$ the integral (C.7) can be estimated as

$$\int_{11}^{10} \sqrt{\frac{X}{Y}} e^{-in\theta} d\theta \approx -ie^{-in\beta} \int_0^\infty t^{1/2} e^{-nt} dt \times \sqrt{\frac{(1+\chi e^{i\beta})e^{i\beta}(e^{i\beta}-e^{-i\beta})}{(\chi e^{i\beta}-1)(e^{i\beta}-y_3)(e^{i\beta}-y_4)}} = -\frac{ie^{-in\beta}}{2n^{3/2}} \times \sqrt{\frac{\pi(1+\chi e^{i\beta})\sin\beta}{(\chi e^{i\beta}-1)\left(\sin\beta - \frac{i}{2}(\chi^{-1}-\chi)\cos\alpha\right)}}. \quad (C.8)$$

The integral $\int_6^5$ can be estimated in a similar way. It can easily be verified that

$$\int_{11}^{10} - \int_6^5 = 2\mathrm{Re}\int_{11}^{10} = -\frac{\left(1-\frac{1}{4}(\chi^{-1}+\chi)^2\cos^2\alpha\right)^{1/4}}{\sin\frac{\alpha}{2}} \times \sqrt{\frac{\pi}{2n^3}} \times \cos\left(n\beta - \frac{\rho}{2}\right), \quad (C.9)$$

where

$$\rho = \arctan\frac{1+\frac{1}{4}(\chi^{-1}+\chi)^2\cos\alpha}{\frac{1}{2}|\chi^{-1}-\chi|\sqrt{1-\frac{1}{4}(\chi^{-1}+\chi)^2\cos^2\alpha}}. \quad (C.10)$$

Thus, the final expression for the analytical approximation of the x component of echo amplitudes for $\cos\alpha > 0$ is as follows:

$$\frac{M_{xn}}{M_{x0}}(\xi_1\xi_2)^{-n/2} \approx \frac{b^n}{2}\sqrt{\frac{(b+\chi)(1-2b\cos\beta+b^2)}{\chi(b^2+1)}} \times I_0\left[n\frac{b-\chi}{2\chi}\right]\exp\left[-n\frac{b-\chi}{2\chi}\right] + \frac{(-1)^n}{4b^n} \times \sqrt{\frac{(1+2b\cos\beta+b^2)b\chi}{(1+\chi b)(b^2+1)}} \times \frac{1-\chi b}{\chi b}\left\{ I_0\left[n\frac{1-\chi b}{2\chi b}\right] + I_1\left[n\frac{1-\chi b}{2\chi b}\right]\right\}\exp\left[-n\frac{1-\chi b}{2\chi b}\right] - \frac{\left(1-\frac{1}{4}(\chi^{-1}+\chi)^2\cos^2\alpha\right)^{1/4}}{2\sqrt{2\pi n^3}\sin\frac{\alpha}{2}}\cos\left(n\beta - \frac{\rho}{2}\right), \quad (C.11)$$

where

$$b = \frac{1}{2}|(\chi^{-1}-\chi)\cos\alpha| + \sqrt{\frac{1}{4}(\chi^{-1}-\chi)^2\cos^2\alpha + 1}. \quad (C.12)$$

Combining Eq. (C.11) with the case $\cos\alpha < 0$ considered in a similar way, one obtains Eq. (54).

Appendix D. Derivation of the analytic approximation (69)

For $\chi \leqslant (1-\sin\alpha)/|\cos\alpha| \leqslant 1$, $0 \leqslant \alpha \leqslant \pi$, $\alpha \neq \pi/2$ all roots (B.3) are real. We first assume that $\cos\alpha > 0$, since the case $\cos\alpha < 0$ can be treated in a similar way. Taking $y = e^{i\theta}$ in Eq. (B.2), one obtains Eq. (C.1). Let us change the integration path to that shown in Fig. 5. When by-passing the branch points, the radical phase changes should be taken into account, as shown in the same figure (we will treat the x component only, since the y one can be treated in a similar way). Taking into account the direction of integration as well, it can readily be verified that only the following integrals contribute to the integral in Eq. (C.1):

$$\int_{-\pi}^{\pi} = 2\left\{\int_{7'}^{6'} + \int_{9'}^{8'} - \int_{12'}^{11'}\right\} \quad (D.1)$$

(the indices denote the direction of integration, all integrals mean principal values, primes in the integrals indicate that the corresponding integration contour is that shown in Fig. 5, not in Fig. 4). The integral $\int_{12'}^{11'}$ is the same as in Eq. (C.5), and the estimation is the same, too (Eq. (C.6)). Let us consider each of the remaining integrals separately.

Taking $\theta = -i\ln y_1 - it$, the integral $\int_{7'}^{6'}$ can be rewritten as:

$$\int_{7'}^{6'} \sqrt{\frac{X}{Y}} e^{-in\theta} d\theta = -\frac{ie^{-i\pi/2}}{y_1^n} \times \int_0^{-\ln(\chi y_1)} \sqrt{\frac{(1+\chi y_1 e^t)y_1(e^t-1)(y_1 e^t - y_2)}{(1-\chi y_1 e^t)(y_1 e^t - y_3)(y_1 e^t - y_4)}} e^{-nt} dt \approx -\frac{1}{y_1^n}\sqrt{\frac{(\chi^{-1}+y_1)(y_1-y_2)}{(y_1-y_4)(y_1-y_3)}} \int_0^{y_2\chi^{-1}-1} \frac{t^{1/2}e^{-nt}}{(y_2\chi^{-1}-1-t)^{1/2}} dt = -\frac{\pi(y_2\chi^{-1}-1)}{2y_1^n}\sqrt{\frac{(\chi^{-1}+y_1)(y_1-y_2)}{(y_1-y_4)(y_1-y_3)}} \times \left\{ I_0\left[n\frac{y_2-\chi}{2\chi}\right] - I_1\left[n\frac{y_2-\chi}{2\chi}\right]\right\}\exp\left[-n\frac{y_2-\chi}{2\chi}\right]. \quad (D.2)$$

Taking $\theta = -i\ln y_3 - it$, the integral $\int_{9'}^{8'}$ can be estimated in a similar way:

$$\int_{9'}^{8'}\sqrt{\frac{X(e^{i\theta})}{Y(e^{i\theta})}}e^{-in\theta}\,d\theta=-\frac{ie^{i\pi/2}}{y_3^n}$$
$$\times\int_0^{\ln(-y_2y_4)}\sqrt{\frac{(\chi^{-1}+y_3e^t)(y_1-y_3e^t)(y_2-y_3e^t)}{(\chi^{-1}-y_3e^t)y_3(e^t-1)(y_3e^t-y_4)}}e^{-nt}dt$$
$$\approx\frac{1}{y_3^n}\sqrt{\frac{(\chi^{-1}+y_3)(y_1-y_3)}{(\chi^{-1}-y_3)(y_3-y_4)}}\int_0^{-y_2y_4-1}\frac{(-y_2y_4-1-t)^{1/2}}{t^{1/2}}e^{-nt}dt$$
$$=\frac{\pi(-y_2y_4-1)}{2y_3^n}\sqrt{\frac{(\chi^{-1}+y_3)(y_1-y_3)}{(\chi^{-1}-y_3)(y_3-y_4)}}\times\left\{I_0\left[n\frac{-y_2y_4-1}{2}\right]\right.$$
$$\left.+I_1\left[n\frac{-y_2y_4-1}{2}\right]\right\}\exp\left[-n\frac{-y_2y_4-1}{2}\right].\qquad\text{(D.3)}$$

Thus, the final expression for the analytical approximation for the x component of echo amplitudes for $\chi\leqslant(1-\sin\alpha)/|\cos\alpha|\leqslant 1$ and $\cos\alpha>0$ is as follows:

$$\frac{M_{xn}}{M_{x0}}(\xi_1\xi_2)^{-n/2}\approx\frac{b^n(bc-1)}{4}\sqrt{\frac{(b+\chi)(b-c)}{(b-\chi)(b^2+1)c}}\times\left\{I_0\left[\frac{n(bc-1)}{2}\right]\right.$$
$$\left.+I_1\left[\frac{n(bc-1)}{2}\right]\right\}\exp\left[-n\frac{bc-1}{2}\right]$$
$$-\frac{c^n}{4}\frac{c-\chi}{\chi}\sqrt{\frac{(c+\chi)(1-c^2)b}{(b-c)(1+bc)\chi}}\times\left\{I_0\left[n\frac{c-\chi}{2\chi}\right]\right.$$
$$\left.-I_1\left[n\frac{c-\chi}{2\chi}\right]\right\}\exp\left[-n\frac{c-\chi}{2\chi}\right]$$
$$+\frac{(-1)^n}{4b^n}\frac{1-\chi b}{\chi b}\sqrt{\frac{(b+c)(1+bc)\chi b}{(1+\chi b)(1+b^2)c}}$$
$$\times\left\{I_0\left[n\frac{(1-\chi b)}{2\chi b}\right]+I_1\left[n\frac{(1-\chi b)}{2\chi b}\right]\right\}\exp\left[-n\frac{(1-\chi b)}{2\chi b}\right],\quad\text{(D.4)}$$

where

$$c=\frac{1}{2}(\chi^{-1}+\chi)|\cos\alpha|-\sqrt{\frac{1}{4}(\chi^{-1}+\chi)^2\cos^2\alpha-1}\qquad\text{(D.5)}$$

and b is the same as in (C.12). Combining Eq. (D.4) with the case $\cos\alpha<0$ considered in a similar way, one obtains Eq. (69).

References

[1] I.V. Koptyug, R.Z. Sagdeev, Non-traditional applications of NMR tomography, Russ. Chem. Rev. 72 (2003) 183–212.

[2] I.V. Koptyug, R.Z. Sagdeev, Applications of NMR tomography to mass transfer studies, Russ. Chem. Rev. 71 (2002) 899–948.

[3] I.V. Koptyug, R.Z. Sagdeev, Modern applications of NMR tomography in physical chemistry. The characteristic features of the technique and its applications to studies of liquid-containing objects, Russ. Chem. Rev. 71 (2002) 672–699.

[4] J. Hennig, Multiecho imaging sequences with low refocusing flip angles, J. Magn. Reson. 78 (1988) 397–407.

[5] J. Hennig, Echoes – how to generate, recognize, use or avoid them in MR-imaging sequences, Concepts Magn. Reson. 125 (1991) 114–119.

[6] T.C. Mills, D.A. Ortendahl, N.M. Hylton, L.E. Crooks, J.W. Carlson, L. Kaufman, Partial flip angle MR imaging, Radiology 162 (1987) 531–539.

[7] G.R. Coates, L. Xiao, M.G. Prammer, NMR Logging Principles and Applications, Halliburton Energy Services, Houston, 1999.

[8] G. Goelman, M.G. Prammer, The CPMG pulse sequence in strong magnetic field gradients with application to oil-well logging, J. Magn. Reson. A 113 (1995) 11–18.

[9] T.E. Bull, Effect of RF inhomogeneities on spin-echo measurments, Rev. Sci. Instrum. 45 (1974) 232–242.

[10] M.D. Hürlimann, D.D. Griffin, Spin dynamics of Carr–Purcell–Meiboom–Gill-like sequences in grossly inhomogeneous B_0 and B_1 fields and application to NMR well logging, J. Magn. Reson. 143 (2000) 120–135.

[11] Yu. Zur, An algorithm to calculate the NMR signal of a multi spin-echo sequence with relaxation and spin–diffusion, J. Magn. Reson. 171 (2004) 97–106.

[12] N.N. Lukzen, A.A. Savelov, Analytical derivation of multiple spin echo amplitudes with arbitrary refocusing angle, J. Magn. Reson. 185 (2007) 71–76.

[13] N.N. Lukzen, M.V. Petrova, I.V. Koptyug, A.A. Savelov, R.Z. Sagdeev, The generating functions formalism for the analysis of spin response to the periodic trains of RF pulses. Echo sequences with arbitrary refocusing angles and resonance offsets, J. Magn. Reson. 196 (2009) 164–169.

[14] A. Korn, M. Korn, Mathematical Handbook for Scientists and Engineers, McGraw-Hill Book Company Inc., New York/Toronto/London, 1961.

[15] F. Bălibanu, K. Hailu, R. Eymael, D.E. Demco, B. Blümich, Nuclear magnetic resonance in inhomogeneous magnetic fields, J. Magn. Reson. 145 (2000) 246–258.

[16] D.E. Freed, M.D. Hürlimann, U.M. Scheven, The equivalence between off-resonance and on-resonance pulse sequences and its application to steady-state free precession with diffusion in inhomogeneous fields, J. Magn. Reson. 162 (2003) 328–335.

[17] A.D. Bain, E.W. Randall, Hahn spin echoes in large static gradients following a series of 90° pulses, J. Magn. Reson. 123 (1996) 49–55.

[18] M.B. Franzoni, P.R. Levstein, Manifestations of the absence of spin diffusion in multipulse NMR experiments on diluted dipolar solids, Phys. Rev. B 72 (2005) 235410-1–235410-5.

[19] M.B. Franzoni, P.R. Levstein, J. Raya, J. Hirschinger, Hole burning in polycrystalline C_{60}: an answer to the long pseudocoherent tails, Phys. Rev. B 78 (2008) 115407-1–115407-5.

[20] M.H. Levitt, Spin Dynamics: Basics of Nuclear Magnetic Resonance, second ed., Wiley, 2008.